Preliminary Geothermal Conceptual Model at Dabeiba-Antioquia, Colombia

Nicolas Montoya Londoño
Maria Camila Parra Londoño

Trabajo de grado presentado como requisito parcial para optar al título de Geólog@

Asesora:
Ingeniera Geóloga María Isabel Marín Cerón, PhD

UNIVERSIDAD EAFIT
ESCUELA DE CIENCIAS
DEPARTAMENTO DE CIENCIAS DE LA TIERRA
GEOLOGIA
MEDELLIN

AGRADECIMIENTOS

A nuestras familias, unidas por demás, a quienes les debemos todo lo que somos y seremos. A la Universidad EAFIT, especialmente a la Escuela de Ciencias y su Departamento de Geología, por apoyo logístico y administrativo durante todos los años de formación académica. A la docente Maria Isabel Marín Cerón, por su paciencia y constante retroalimentación académica, profesional y personal.

A la ingeniera Manuela Botero y el equipo de trabajo de la Universidad Nacional de Colombia, por sus diferentes contribuciones previas a la realización de este proyecto investigativo. A la empresa SHI S.A.S, por el tiempo y los recursos implementados en la sección hidrogeológica del artículo, especialmente al ingeniero Breiner Dan Bastidas. A la geóloga Adriana Londoño por su apoyo en la compilación y organización de las bases de datos.

בהופעה שלך.עשה דברים עם הלב שלך, כך שהסיבה נכונה

"Investigar es ver lo que todo el mundo ha visto, y pensar lo que nadie más ha pensado".

Albert Szent-Györgyi

PREFACIO

El siguiente trabajo se compone de un artículo investigativo: Preliminary Geothermal Conceptual Model at Dabeiba-Antioquia, Colombia. Es un análisis de índole científico para ser sometido en el Boletín de la Universidad Industrial de Santander.

A partir del análisis de potenciales play geotérmico en Colombia, nos planteamos la siguiente hipótesis de trabajo: El prospecto geotérmico de Dabiba (DGS) es un "play" geotérmico asociado a controles estructurales generados por la zona de sutura de Dabeiba.

Teniendo en cuenta esta hipótesis, nos preguntamos si el DGS es posible de ser entendido a partir de la construcción de un modelo geotérmico conceptual basado en la caracterización estructural, hidrogeológica, hidrogeoquímica y termocronológica con recopilación de información secundaria.

Para poder llevar a cabo este proyecto, se planteó como objetivo general del trabajo construir un modelo geotérmico conceptual, que integró las herramientas de: (1) análisis hidrogeológico e identificación de zonas de recargas, (2) hidrogeoquímica de tres fuentes termales ubicadas sobre la traza de la falla Chimurró y (3) Termometría en las aguas termales y termocronología en los sedimentos de la Formación Guineales para determinar el tipo de play y la dinámica del flujo de calor. Finalmente, para el logro de este objetivo se plantearon los siguientes objetivos específicos:

- Analizar las tendencias estructurales por cada unidad litológica.
- Definir zonas potenciales de recarga de aguas subterráneas, con el fin de construir un modelo hidrogeológico conceptual asociado a las fuentes termales.
- Interpretar de las bases de datos geoquímicas e isotópicas del sistema geotérmico de Dabeiba a partir de las fuentes termales identificadas en el inventario de fuentes termales del Servicio Geológico Colombiano.
- Interpretar datos termocronológicos existentes en la Formación Guineales en relación con el "play" geotérmico.
- Construir un modelo geotérmico conceptual integrando análisis multiherramienta.

TABLA DE CONTENIDO

1. INTRODUCTION 10
2. GEOLOGICAL SETTING 11
2.1. Local Geology 13
3. CONCEPTUAL FRAMEWORK AND METHODOLOGY 14
3.1. Geodatabase for geothermal studies 15
3.2. Structural analyses and preferential directions 19
3.3. Recharge zones 21
3.4. Hydrochemistry analysis 24
3.5. Low temperature thermochronology 25
4. RESULTS 26
4.1. Thematic maps 26
4.1.1. Land Covers 26
4.1.2. Soil types 26
4.1.3. Geology 27
4.1.4. Precipitation 30
4.1.5. Temperature and potential evapotranspiration 30
4.2. Preferential directions 31
4.3. Hydrogeological properties of study area (Recharge zones) 34
4.3.1. Potential recharge model-(hydrometeorological soil´s balance) 34
4.3.2. Parameters and simulations periods 35
4.3.3. Potential zones mapping 36
5. DISCUSSION: GEOTHERMAL CONCEPT MODEL 38
5.1. Hydrochemistry 38
5.2. Mixing model 43
5.3. Heat flow and advection 44
6. CONCLUSIONS 46
7. REFERENCES 48

LISTA DE FIGURAS Y TABLAS

Figure 1. Location of study area. Map 114- Dabeiba, Antioquia. Adapted of INGEOMINAS, 2012. Three hot springs located in the study area; the green star was the Guineales spring, the yellow star the Chobar spring, and the purple star the Mohan spring. 12
Figure 2. Geological units of the study area. Generated from INGEOMINAS, 2012 and Botero 2018. N4N5bb (Button Basalts), K2cn (Cañas Gordas complex-Nutibara member), K2bb (Diabase of San José de Urama), K2alu (Cañas Gordas complex-Urrao member), E1tm (Mandé Batholith), E1tmn (Mandé Batholith Intrusive), E1csce (Santa Cecilia-La Equis complex), E3n1g (Guineales Formation), Q2v (Slope deposits), Q2al (Alluvial deposits). 13
Figure 3. Generalized behavior of the local structural system. Geological units and faults dispositions. Profile direction NW-SE. Adapted from Geomodelr 2016-Version 0.1.18. ... 14
Figure 5. Methodological flowchart of structural analyses. Adapted from (Arken.nmbu.no/qgisplugins, 2019). 20
Figure 6. Rose diagrams types. Directions mean of segments. Adapted from (Arken.nmbu.no/qgisplugins, 2019). 20
Figure 4. Non-magmatic active geothermal play system in extensional terrains with different types of reservoirs (1, 2a and 2b). Type 1 is a convection cell from infiltration to discharge along one fault. Temperature gradient is gradually increasing at wellsite1. Type 2a and 2B are fault leakage controlled plays. The temperature gradient of a well drilled into such an area rises up to the permeable layer and drops below the layer (well 2a and 2b). Adapted from (Moeck, 2014). 22
Figure 7. Methodological flowchart of hydrogeological behavior. Adapted and modified from (Schosinsky N, 2007). 23
Figure 8. Idealized model for calculating recharge. Modified from (Schosinsky N, 2007). 23
Figure 9. Methodological flowchart of the hydro geochemistry. Adapted from (Gómez , 2019). 25
Figure 10. Thematic maps whit physical conditions. a). Land covers, adapted from (CORINE LAND COVER, 2010). b). Geological units, adapted from (Rodriguez, Zapata, & Gomez , 2012). C). Soil types, adapted from (IGAC, 2007). d). Structural patterns, adapted from (Botero G, 2018). 28
Figure 11. Thematic maps whit climatological variables. a) Spatial distribution of precipitation, generated whit a national deriva, proposed by Alvarez, 2007; b) Spatial distribution of mean temperature. c) Spatial distribution of slopes, generated in degrees; d) Potential evapotranspiration distribution, generated whit Cenicafe´s equation. 29
Figure 12. Preferential directions of drainage network for each lithology. Generated from (Arken.nmbu.no/qgisplugins, 2019). 32
Figure 13. Preferential directions of faults and lineaments for each lithology. Generated from (Arken.nmbu.no/qgisplugins, 2019). 33
Figure 14. General tendency of drainage network and lineaments in study area. Generated from (Arken.nmbu.no/qgisplugins, 2019). 34

Figure 15. Annual rainfall cycle for the two base stations. On the left, FUEMIA with a multiannual average of 1561 mm/year; on the right VILLARTEAGA with a multiannual average of 5245 mm/year. 35
Figure 16. Annual evapotranspiration cycle for the two base stations. On the left, MUSINGA with a multiannual average of 1043.1 mm/year; on the right VILLARTEAGA with a multiannual average of 1349.9 mm/year. 36
Figure 17. Spatial distribution of the potential recharge by precipitation for a normal year. 37
Figure 18. Spatial distribution of the potential recharge by precipitation. a) Potential recharge for dry year; b) Potential recharge for dry year. 37
Figure 19. Piper diagram of Dabeiba hot springs. Sodium Chloride type. Mohan spring is represented by an orange dot, Guineales by a blue dot and Chobar by a brown dot..... 38
Figure 20. Stiff´s diagrams of Dabeiba springs. Spatial distribution in geological map. The green diagram represent Guineales spring, the blue diagram represent Chobar spring and the violet diagram represent Mohán spring. 39
Figure 21. Cross-plot of the stable isotopes of water (δ18O – δD). The red line is the segment of the Colombian Meteoric Line (CML) and the gray line is Global Meteoric Water line GWML, the range of andesitic water as proposed by Giggenbach (1992). Dabeiba springs dots reflect a slight rise and to right. Mohan spring is represented by a red dot, Guineales by a green dot and Chobar by an orange dot. Adapted from (Gómez , 2019)..... 40
Figure 22. Plot of conservative elements proposed by Giggenbach (1991). a.) Cl-Li-B Plot; b.) Cl-Sr-B Plot. In two cases Mohan spring is represented by a red dot, Guineales by a green dot and Chobar by an orange dot. Modified by (Gómez , 2019). The plots were made on using the spreadsheet of Liquid Analysis v3 (Powell & Cumming, 2010)..... 41
Figure 23. Na-K-Mg plot, adapted from (Gómez , 2019). Mohan spring is represented by a red dot, Guineales by a green dot and Chobar by an orange dot. The plots were made on using the spreadsheet of Liquid Analysis v3 (Powell & Cumming, 2010)..... 42
Figure 24. Geothermal conceptual model #1. Behavior of the surface system. 44
Figure 25. Block diagram adapted from Ehlers et al. (2001) and (Gorynski K. , Walker, Stockli, & Sabin, 2014), showing the thermal characterization of normal faults where isotherms, represented here as the AHe partial retention zone (PRZ), are advected upward in rapidly exhumed footwalls of normal faults. Adjusted to structural system of Dabeiba. 45
Figure 26. Geothermometers map and comparative samples with ages U-T-He in apatite. The yellow dot represent Guineales spring; the orange dot represents Chobar spring; the red spring represent Mohan spring. 46
Figure 27. Geothermal conceptual model #2. Behavior of mixing process and heat source. 47

Table 1. Data set summary of the information collected, and used in the different topics involved. 16
Table 2. Major chemical constituents, pH and the temperature of thermal waters from Dabeiba. The species of the solution in Mg/L. Taken and adapted from (Gómez , 2019). . 24

Table 3. Summarized simulation periods based in FUEMIA station and VILLARTEAGA station. 35
Table 4. Summarized simulation periods of evapotranspiration based in MUSINGA station and VILLARTEAGA station. 36
Table 5. Reservoir temperatures (°C) estimated by solute geothermometers in Dabeiba thermal springs. Taken from (Gómez , 2019). 42

Preliminary Geothermal Conceptual Model at Dabeiba-Antioquia, Colombia

Montoya Londoño Nicolás, Parra Londoño Maria Camila, Marín-Cerón María Isabel, Gómez Esteban
Department of earth sciences Universidad EAFIT. Medellin, Colombia
nmonto13@eafit.edu.co ; mparral@eafit.edu.co ; mmarince@eafit.edu.co

ABSTRACT

The Dabeiba geothermal system (DGS) corresponds to an extensional character "play". It is located on the westernmost side of the western mountain range, in the subregion of Urabá, Antioquia-Colombia; where heat flow occurs along the Dabeiba-Pueblo Rico fault system.

This structural system puts the Cañasgordas Complex lithology, the Guineal Formation and rocks from the Santa Cecilia-La Equis Complex in contact from East to North. The Chimurro fault, of normal character, raised the geothermal gradient of the area, evidenced in the presence of three hydrothermal sources: the Mohán spring, Chobar spring and Guineales spring.

The DGS can be understood from the construction of a conceptual geothermal model based on structural, hydrogeological, hydrogeochemical and thermochronological characterization from the collection of secondary information. Using a semi-distributed water balance model, the potential recharge zones and the relationship with the structural trends of the area were estimated. This was done by identifying the infiltration potential to the West of the area as responsible for the entry of meteoric water into the system, favoring the formation of sodium-chlorinated waters with a tendency of mixing evidenced in the isotopic data.

The conceptual geothermal model interprets the heat flow from a deep source associated with isothermal advection processes generated by the normal Chimurro fault, along the Guineal Formation. Through the analysis of geothermometers together with the low temperature thermochronological data ((U/Th) He in apatites) in the sediments of the Guineal Formation, it was possible to classify the DGS as a low enthalpy play with an approximate temperature

of 150 ± 30 ° C. Additionally, it is suggested that hydrothermal fluids along the Chimurro fault networks may have been operating from 1.7 to 2 Ma until now.

RESUMEN

El sistema geotérmico de Dabeiba (DGS) corresponde a un “play” de carácter extensional localizado sobre el costado más occidental de la cordillera occidental, en la subregión del Urabá, Antioquia-Colombia; donde el flujo de calor ocurre a lo largo del sistema de fallas Dabeiba-Pueblo Rico. Dicho sistema estructural, pone en contacto litologías del Complejo Cañasgordas, la Formación Guineales y rocas del Complejo Santa Cecilia-La Equis de Este a Norte. La falla Chimurró de carácter normal, elevó el gradiente geotérmico del área, evidenciado en la presencia de tres fuentes hidrotermales: El manantial de Mohán, manantial Chobar y manantial Guineales.

El DGS puede ser entendido a partir de la construcción de un modelo geotérmico conceptual basado en la caracterización estructural, hidrogeológica, hidrogeoquímica y termocronológica a partir de recopilación de información secundaria. Usando un modelo semi-distribuido de balance hídrico, se estimaron las zonas potenciales de recarga y la relación con las tendencias estructurales del área, asociando el potencial de infiltración que se presenta al Oeste de la zona como el responsable de la entrada de agua meteórica en el sistema, favoreciendo la formación de aguas sódico-cloruradas con una tendencia de mezcla evidenciada en los datos isotópicos.

El modelo geotérmico conceptual interpreta el flujo de calor desde una fuente profunda asociada a procesos de advección isotérmica generados por la falla normal Chimurro, a lo largo de la Formación Guineales. Mediante el análisis de geotermómetros junto con los datos termocronológicos de baja temperatura ((U / Th) He en apatitos) en los sedimentos de la Formación Guineales, fue posible clasificar el DGS como un “play” de baja entalpía con una temperatura aproximada de 150 ± 30 ° C. Adicionalmente, se sugiere que los fluidos hidrotermales a lo largo de las redes de fallas de Chimuro pueden haber estado actuando desde 1.7 a 2 Ma hasta el presente.

1. INTRODUCTION

A geothermal system may be encountered in diverse geologic environments and theoretically all over the world, mainly related to a convergent tectonic plate setting, which has a fundamental influence on the characteristics of a geothermal play. The thermal and hydrogeological regime, heat flow, fluid dynamics, fluid chemistry, faults and fractures, stress regime and lithological sequence are all controlled by the plate tectonic framework and are critical for understanding the geothermal play system (Moeck, 2014).

Some basic parameters have been defined for a better understanding of the geothermal exploration such as: geological-structural characterization, hydrogeological, and geophysical studies together with hydro-chemical analysis of spring waters. In general, the hydrothermal activity depends on numerous factors including the understanding of fluids circulation, the heat source and Pathways (Setyawan, Yudianto, Nishijama, & Hakim, 2015). Therefore, a combination of a multi-technique approach with a suite of modern site-specific exploration techniques is required to present a preliminary geothermal conceptual model (Kenya & Oham, 2009) for a deep understanding of the geologic controls of the play (Moeck, 2014).

In this study we have chosen the Dabeiba geothermal system (DGS) as a target area to understand a non-magmatic convection-dominated play. The tectonic context of the North-western corner of Colombia is characterized by a high geological complexity due to the interaction of three main tectonic plates, Nazca-Farallón, Caribe, and Sur America; and at least two major cortical blocks (Andes del Norte and Panamá-Chocó) (Duque-Caro, 1990). This area, is a purely fault controlled play system related to a fractured medium, where the flow convection may occur along the regional faults (e.g. Chimuro fault-Dabeiba-Pueblorico System) and groundwater may be mixed with meteoric water (Reed , 1982).

To propose a preliminary Geothermal Conceptual Model of DGS, we use a multi-tool study that involves a hydrological conceptual model and hydrochemistry analysis from the Colombian Geological Survey Spring Water Geodatabase (Servicio Geológico Colombiano SGC, 2014). We used this study to understand the spatial distribution of recharge zones, transit and discharge; and the mixture of different types of water along the Dabeiba-Pueblorico Suture zone, specifically close to the Chimurró normal fault (Rodriguez, Zapata,

& Gomez, 2012). Here, we expect that the geothermal gradient may raise in the footwalls via isotherm advection (e.g. Ehlers and Chapman, 1999), highlighting a ¨blind¨ geothermal system. The thermal springs we analyzed at the study area are Guineales, Chobar, and Mohán springs (**Figure 1**).

2. GEOLOGICAL SETTING

The study area is located on the geological map 114-Dabeiba, Antioquia (Rodriguez, Zapata, & Gomez, 2012), to the Northwest of Medellín, on the northern part of the Western Cordillera of Colombia, along the Vía al Mar route to the Urabá region (Figure 1). The tectonic setting in this region is associated with the triple junction of the Nazca, Caribbean, and South American plates which result in a large and deformed litho-tectonic blocks mosaic-like arrangement limited by faults in a regional N-S trending (Rodríguez & Zapata, 2012). This resulting tectonics between two regional blocks, generates a mosaic of deformed rocks constituted are the Chocó-Panama Block (PCB) and the Cañas Gordas Block (CGB). The Chocó-Panama Block in Colombia is constituted by the Batolito de Mandé (Álvarez J. , 1970), the Santa Cecilia-La Equis Complex (Calle & Salinas, 1986), and Cañas Gordas Block.The latter is constituted by a basement of oceanic affinity basaltic composition T-MORB, represented by the Barroso formation (Rodríguez & Arango, 2013) and a set of Cretaceous sedimentary units, known as Penderisco Formation (Álvarez & Gonzalez, 1978) (***Figure 2***).

Structurally, the NW of South America is dominated by fault systems with transpressive characteristics, with an important movement along the NS course, following the general Romeral fault system (RFS) and the Dabeiba Pueblo Rico fault system trends (DPRFS) (Rodriguez, Zapata, & Gomez, 2012) (Botero G, 2018). These two systems are considered the main sutures defining the dominant structural trend and regime within the study area. Those systems are locally represented by Cañas Gordas, Chimurro and Cerrazón Fault from West to East (Rodríguez & Zapata, 2012), also controlling the lithological contacts.

Three thermal springs were chosen: the Guineales spring, located close to Riosucio River, around 12 km from Dabeiba town. Outcropping on the hillside is the Chobar spring, approximately 3 kilometers away from the Northwest of the Urabá road. Finally, the Mohán

spring is the southernmost point, located near the Mohán School, about four hours away by foot.

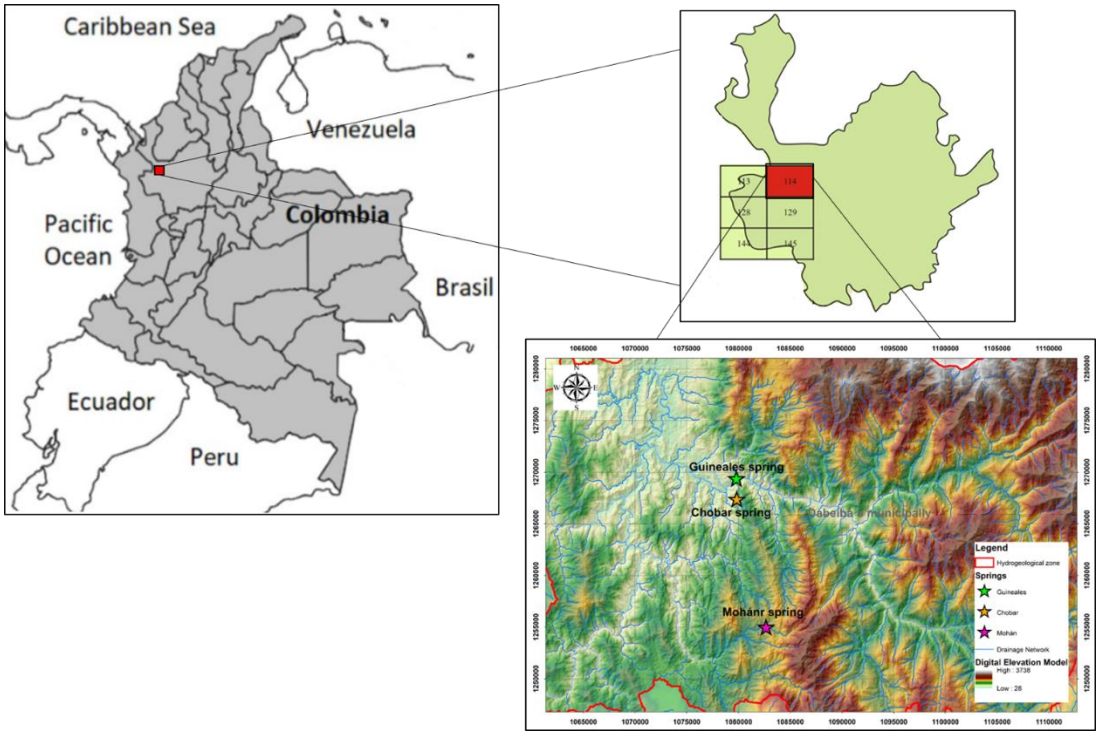

Figure 1. Location of study area. Map 114- Dabeiba, Antioquia. Adapted of INGEOMINAS, 2012. Three hot springs located in the study area; the green star is the Guineales spring, the yellow star the Chobar spring, and the purple star the Mohan spring.

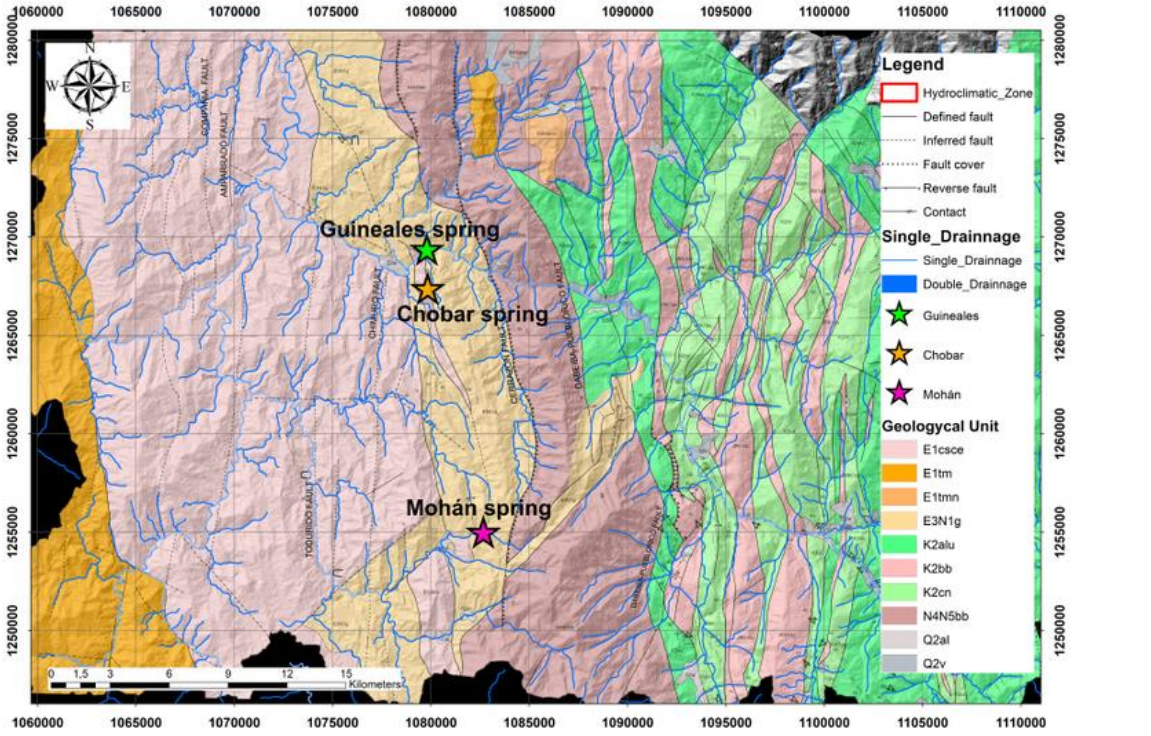

Figure 2. Geological units of the study area. Generated from INGEOMINAS, 2012 and Botero 2018. N4N5bb (Button Basalts), K2cn (Cañas Gordas complex-Nutibara member), K2bb (Diabase of San José de Urama), K2alu (Cañas Gordas complex-Urrao member), E1tm (Mandé Batholith), E1tmn (Mandé Batholith Intrusive), E1csce (Santa Cecilia-La Equis complex), E3n1g (Guineales Formation), Q2v (Slope deposits), Q2al (Alluvial deposits).

2.1. Local Geology

The lithological units that outcrop in the study area from East to West are the Cretaceous sedimentary rocks of the Penderisco Formation (K2alu) (Álvarez & Gonzalez, 1978). These are in fault contact with the Guineales Formation (E3N1g) (Servicio Geológico Colombiano SGC, 2014) and the Barroso formation (K2bb). The thermal springs are located between the Chimurró faults to the West and the La Cerrazón fault to the East. The latter are part of the Amparradó - Murindó Failure System initially described by Mejía & Salazar (2007), and comprising a series of NS structures, affecting the rocks of the Santa Cecilia-La Equis Complex and the Guineales Formation. This geological unit formation forms an irregular strip with general direction S-N trend, and 2 to 3 km of width. It forms a monoclinal with arrangement N 10 to 23 ° W dipping 53 to 70 ° E on average. It extends from the Togoridó River to the South and continues to the North, following the direction of Riosucio River until Mutatá town (Rodriguez, Zapata, & Gomez, 2012). (See Annex_01_GDB_MontoyaParra/03_MXD/ Geology_1_80.000).

The Guineales Formation is strongly influenced by the DPFS. This fault system shows normal, inverse, and occasional thrusts movements, with sinextral displacements (Rodriguez, Zapata, & Gomez, 2012). The Cerrazón Fault is related to a thrust fault with east vergence. This fault is the contact between the Guineales Formation and the Santa Cecilia-La Equis Complex (Botero G, 2018). The Cerrazón Fault is described by (Rodriguez, Zapata, & Gomez, 2012) as a riding fault with vergence to the East, which puts the Guineales Formation in contact with the Santa Cecilia – La Equis Complex with a plane of failure with a dip near 60 degrees. The Chimurro fault is interpreted as a series of overlapping faults in a N-S direction, which control the Riosucio river to the North, towards the Mutatá town, with a approximate vertical dip of 90°(See Annex_01_GDB_MontoyaParra/03_MXD/ Estructural_Geology_1:80.000). The behavior about the local structural system is shown in the **Figure 3**.

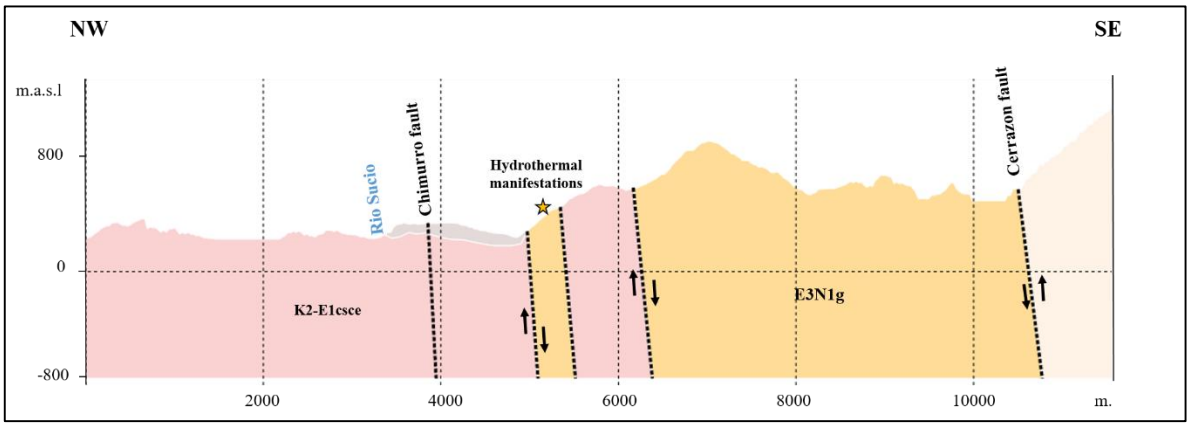

Figure 3. Generalized behavior of the local structural system. Geological units and faults dispositions. Profile direction NW-SE. *Adapted from Geomodelr 2016-Version 0.1.18.*

3. CONCEPTUAL FRAMEWORK AND METHODOLOGY

Geothermal favorability maps in Colombia provide an easy way to access the geothermal resources along the active volcanic fields (e.g. Ruiz volcano, Puracé-Dona Juana), where the surface manifestations of hydrothermal activity are obviously related to the magmatic heat flow. Therefore, geothermal resources have been evaluated only along this magmatic-geothermal system and the so-called "blind" geothermal systems are unexplored and represent an exploration challenge (Gorynski K. , Walker, Stockli , & Sabin, 2014).

The recent volcanism is highly extended in the North Andean Block (Rodríguez & Arango, 2013), showing that the heat in magmatic-type systems is provided by the interaction of shallow meteoric waters (e.g. Ruiz volcano). The complexity associated to structurally complex zones (i.e., cross faults, transfer zones, accommodation zones, ramps, and releasing bends), is not well understood. Moreover, in a non-conventional extensional-type geothermal system the heat flow is not commonly associated with magmatism.

Several studies have been done in the United States of America (e.g. Blackwell, 1983; Wisian et al., 1999; Wisian and Blackwell, 2004; Walker et al., 2005). Those studies point out that the heat flow is related to high background localized advection in the footwalls of normal faults, and deep circulation of hydrothermal fluids along associated range-front faults. Those zones have an increased structural permeability and localized, rapid exhumation (Glazner et al., 1994; Barton et al., 1998; Walker and Whitmarsh, 1998; Caskey and Wesnousky, 2000; Micklethwaite and Cox, 2004; Wisian and Blackwell, 2004; Walker et al., 2005; Faulds et al., 2006; Hickman et al., 2009; Gorynski et al., 2010). In fault-leakage controlled play systems, the fluid leaks from the fault into a permeable concealed layer. In turn, fluids can move from a permeable layer into the fault zone and from there to the surface (***Figure 6)***.
To understand the conceptual model and its methodology, this section has been divided into five sections: (1) Geodatabase for geothermal studies; (2) Structural analyses and preferential directions; (3) Recharge zones; (4) Hydrochemistry and thermometry; and (5) Low Temperature Thermocronology in geothermal studies.

3.1. Geodatabase for geothermal studies

The construction of a geographic database for geothermal studies is a very important issue for the generation of thematic maps that allows the understanding of unconventional geothermal systems. The **Table 1**. summarizes the secondary information for each annex (See Annex_01_GDB_MontoyaParra/06_MXD/ Procesamiento/00_Tablas_Informe).

Table 1. Data set summary of the information collected, and used in the different topics involved.

STRUCTURAL ANALYSIS			
Information	***Thematic source***	***Description***	***Product***
Digital Elevation Model	SIG Government of Antioquia	Digital elevation model As an input for the generation of spatial variables.	Automatic lineaments, spatial variables and adjust climatic model
Structural network	SGC (2012) and Botero (2018)	Cartography of regional structures and associated structural analysis	Regional behavior, particular units structural analyses
Geology	SGC (2012)	Lithological units involved in the study area, structural system and geochemistry.	Extension of the units and shapefiles with spatial properties
Hot spring mapping	SGC (2012)	Location and physical-chemical description of the three thermal sources of the Dabeiba thermal system	Dataset, springs description, shapefiles with spatial properties
RECHARGE MODEL			
Precipitation	IDEAM (1975-2018)	Historical series of daily rainfall to build the annual cycle (1975-2018).	Daily dataset, monthly cycle, interpolation raster.
Potential evapotranspiration	IDEAM (1975-2018)	Values of potential evapotranspiration in monthly values (1975-2018).	Daily log, minimum and maximum temperature, spatial reference files.
National Derive	Alvarez (1977)	Map of spatial distribution throughout the territory of coverage of the national network of meteorological stations	Raster to control the rainfall and evapotranspiration interpolation
Soils	IGAC (2010)	Soil classification units (SCU), for the identification of textural parameters.	Weathering profiles, texture indices and particle size coefficients
Landover	CORINE LAND COVER (2012)	Second level land cover's, for the processing of infiltration.	Type of vegetation, root depth, permanent wilting point and infiltration coefficients
HYDROCHEMISTRY			
National Inventory of Hot Springs	SGC (2012)	Location and detailed description of the hydrothermal sources of the Colombian territory	Composition of major elements, isotopic concentration and conservative elements
Assessment the Hydro geochemistry of Thermal Waters	Gómez (2018)	Dabeiba thermal system evaluation through hydro geochemistry	Compositional diagrams, isotopic relationships, geothermometers and analysis of conservative elements

STRUCTURAL ANALYSIS			
Information	***Thematic source***	***Description***	***Product***
LOW T° THERMOCRONOLOGY			
Low temperature thermo chronology analysis	Botero (2018)	Data and analyses of ((U-Th)/He in Apatite	3 radiometric dating with system reset ages

To compile the data set, we divided it into five types of information:

(1) Hydrochemical data set:

The hydrochemistry database is formed by data from the National Inventory of Hot Springs (e.g. SGC, 2012), the hydrochemical (elemental and isotopic compositions: $\delta^{18}O$ and δD) and in situ parameters (e.g. piper and stiff diagram).This database corresponds to specific coordinates of each point and all the cartographic index for the regional context. In this case the localization of Guineales, Mohán and Chobar spring.

(4) Structural data set (SGC, 2014; Botero, 2018).

This Database is generated with the locations X, Y, Z of previous studies to generate statistical products that represent the main structural trends. It includes the analyses for each unit separately and its relationship with fault systems. For the structural analyses, we also used the elevation Model (e.g. SIG Government of Antioquia) as an input for generating the spatial variables, and the hot spring mapping (e.g. SGC, 2012) with the location and physicochemical description of the three thermal sources of the Dabeiba thermal system. The geology of the zone (e.g. SGC, 2012) consist in the lithological units that are involved in the study area, it also shows the structural and geochemistry system.

The Structural network (e.g. SGC, 2012) (Botero, 2018) shows the Cartography of regional structures, and its corresponding structural analysis.

(5) Hydroclimatological information (e.g.IDEAM 1975-2018).

From the compilation of climatic data and spatial variables, it is understood the way in which the potential recharge is distributed in the area, and the possible sources of meteorological waters that contribute to the processes of mixing the hot springs. For the recharge model approach, we used the daily rainfall historical series to build the annual cycle (e.g. IDEAM, 1975-2018) and monthly values of potential evapotranspiration (e.g.IDEAM, 1975-2018). We also used Drift maps in interpolation (e.g. Alvarez, 1977), that map the spatial distribution throughout the coverage territory of the national network of meteorological stations; Soil Classification Units (SCU) for the identification of textural parameters (e.g. IGAC, 2010); and finally, the second level land covers for infiltration processing (e.g. CORINE LAND COVER, 2012).

(6) Low Temperature Thermochronology (Botero, 2018)

It allows the identification of reset ages in apatites and zircons and their connection with burial processes and heat flows. The correct differentiation between the advective and convective processes of the system and the assessment of the Hydrogeochemistry of Thermal Waters (Gómez, 2018) allowed the evaluation through hydrogeochemistry of the Dabeiba thermal system.

Low temperature thermo chronology analysis (Botero, 2018) has the data and analyses of (U-Th)/He in Apatite, generating a shapefile file with the location of the samples obtained and the ages of the partial reset.

3.2. Structural analyses and preferential directions

The fractured medium unlike the porous medium has properties like continuity, persistence, opening, and spacing that can be quantified with field work or geoprocessing, understanding its behavior at depth (Singhal & Gupta, 2010). Fractures within the rock mass occur on the surface and extend up to a few tens of meters deep, making its interpretation difficult on the surface.

The permeability architecture in geothermal areas is characterized by the geometry and kinematics of the fault-fracture network (Sibson, 1996 in (Roulleau , et al., 2017). The thermal regimes of extensional tectonic settings are complex in that the geothermal gradient is raised in the footwalls of normal faults via isotherm advection during rapid exhumation and erosion and depressed in the hanging wall by burial and sedimentation (Ehlers and Chapman, 1999 in (Gorynski K. , Walker, Stockli , & Sabin, 2014).

The analysis of the drainage system is an interpretation through the stereographic network in which the regional behavior of the structures is analyzed, giving a notion about the orientation of the regional efforts that acted in the zone (Flórez, Ramírez , & Monsalve, 2012). The drainage direction was obtained from the segmentation of the drain-network in straight-line sections, which are representative to a scale of 1:100.000 ***Figure 4***. (See Annex_01_GDB_MontoyaParra/06_MXD/ Procesamiento/03_AnalisisEstructural).

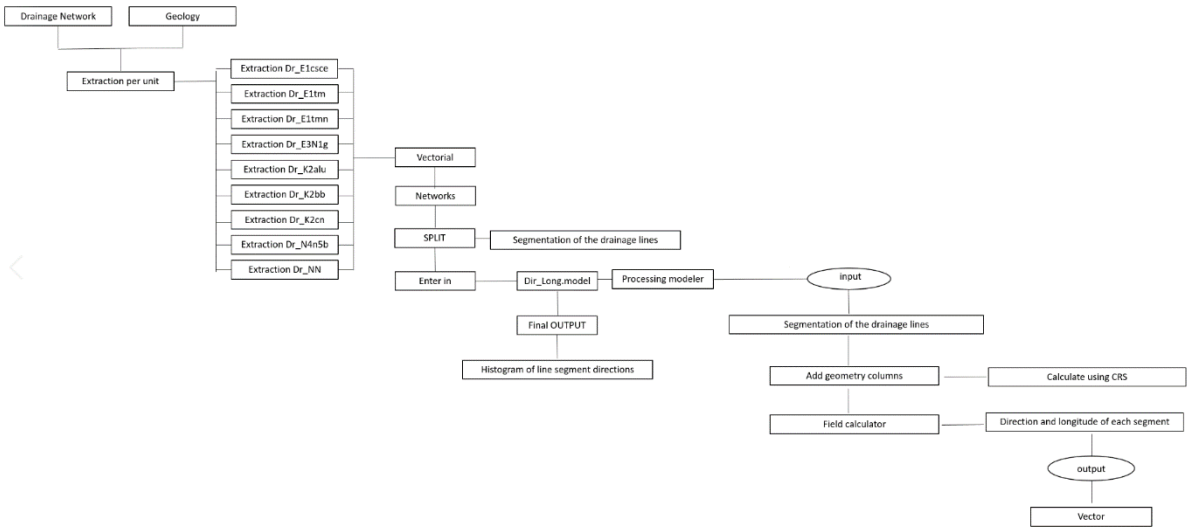

Figure 4. Methodological flowchart of structural analyses. Adapted from *(Arken.nmbu.no/qgisplugins, 2019)*.

The final product was a lineament-direction histogram that indicates the statistical distribution of the hydrological network related to a polygon vector dataset. The accumulated length of line segments is connected to the histogram shape. Alternatively, the number of segments could be used (no weighting on line segment length). The main direction is shown in the rose diagrams (***Figure 5***).

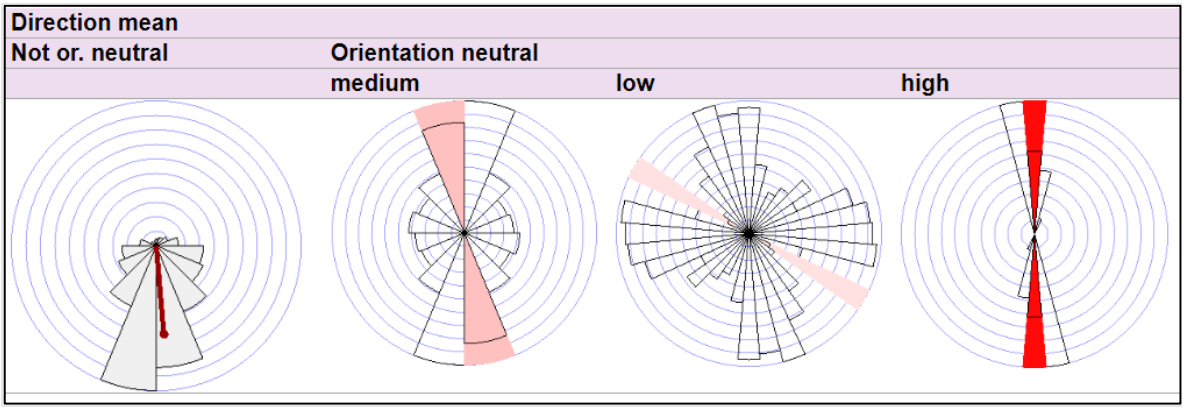

Figure 5. Rose diagrams types. Directions mean of segments. Adapted from *(Arken.nmbu.no/qgisplugins, 2019)*.

The displayed histogram is normalized, so that the maximum value of the direction bins will result in a sector with a maximum length, and the lengths of the sectors of the rest of the bins are scaled proportionally. The mean direction is found by calculating the magnitude of the "direction trend" for each of the bins (Arken.nmbu.no/qgisplugins, 2019).

The value is then normalized to a scale of [0.1] using the sum of the values of bin (total_sum) as the maximum value, and the value that was obtained (even_dist_value) if the distribution of the line of segment lengths between the bins has been like the minimum value. This processing follows ***Equation 1***.

$$normalised\_value = \frac{value - even\_dist\_value}{total\_sum - even\_dist\_value}$$

Equation 1. Normalized value equation. Line direction analyses adapted from *(Arken.nmbu.no/qgisplugins, 2019)*.

3.3. Recharge zones

The stratigraphy, permeability, and fracture pattern of the study area are fundamental factors to model the geothermal system. The hydrogeological properties of the study area were reviewed based on the stratigraphic units described above with their hydrogeological role (Uzelli et al, 2017). Different authors have defined the recharge as the entry of water into the saturated zone where it becomes part of the groundwater reserves. For this case, the methodology proposed by (Schosinsky N, (2007)) shows an approximation of the recharge potential of the aquifer through a soil moisture balance. This analysis approach implies the construction of a hydrogeological model based in a semi-distributed potential infiltration in the light of the understanding of the meteoric water flow that gives rise to mixing processes.

The recharge estimation consists in quantifying the amount of water that reaches the groundwater reserves and that can be given by different sources. (Lerner, Issar, & Simmers, 1990) classify the type of recharge according to the source that originates it: direct, indirect, lateral, irrigation, and urban recharge. The direct recharge is produced by rain, the indirect recharge is due to the influence of permanent, seasonal, or ephemeral channels.

On the other hand, the lateral recharge is produced by the transmission of water from other aquifers. The potential recharge model needs hydro-climatologic parameters, such as precipitation, evapotranspiration and temperature, and inputs like the Digital Elevation Model (DEM), slopes, land cover, and soil texture maps.

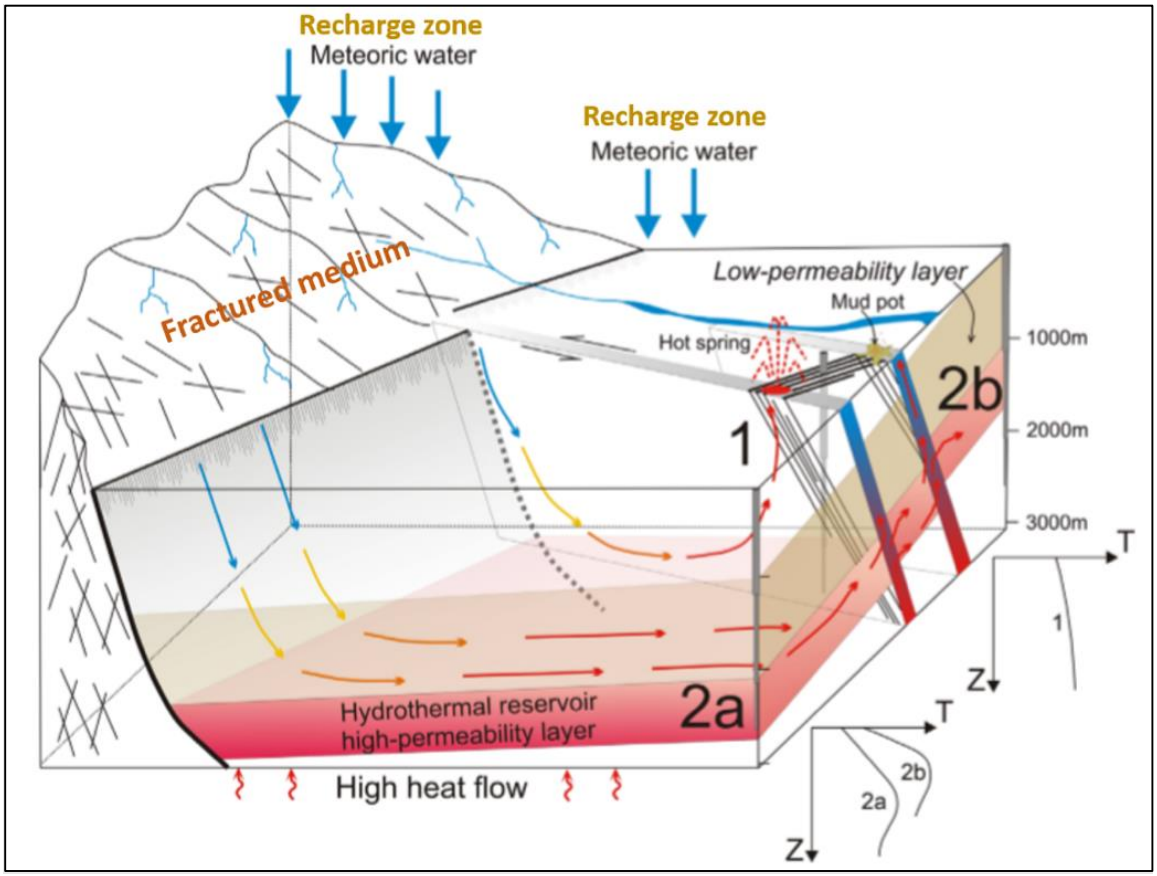

Figure 6. Non-magmatic active geothermal play system in extensional terrains with different types of reservoirs (1, 2a and 2b). Type 1 is a convection cell from infiltration to discharge along one fault. Temperature gradient is gradually increasing at wellsite1. Type 2a and 2B are fault leakage controlled plays. The temperature gradient of a well drilled into such an area rises up to the permeable layer and drops below the layer (well 2a and 2b). Adapted from *(Moeck, 2014)*.

Several thematic maps were generated based on secondary information using ArcGIS 10.5 software. The precipitation and evapotranspiration maps were produced using an external drift interpolation, using data from three hydro-meteorological stations operated by IDEAM. Finally, the potential recharge spatial distribution and the regional flow methodology for mapping recharge zones were obtained by the development of two different models to generate a representative map for potential recharge (magnitude) and recharge zones (map algebra), following the methodological flowchart shown in ***Figure 7***.

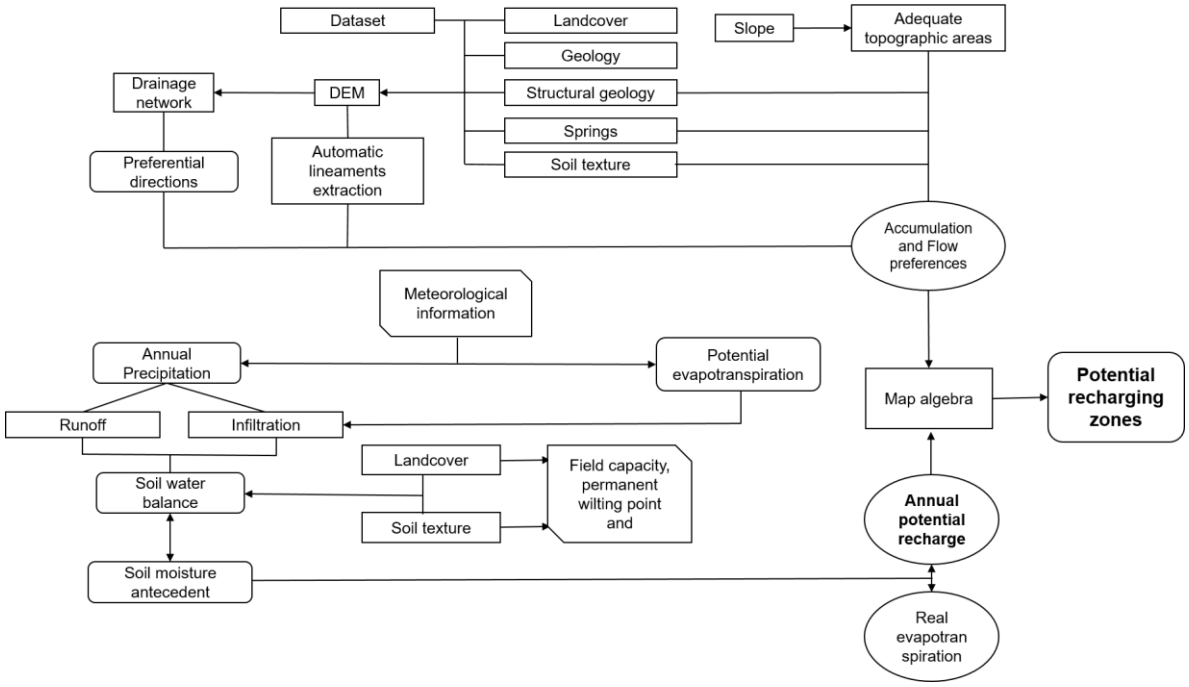

Figure 7. Methodological flowchart of hydrogeological behavior. Adapted and modified from *(Schosinsky N, (2007))*.

The soil-balance study is based on the principle of conservation of matter. That is, the water that enters the floor is equal to the variation of water that is stored in the soil, plus the water that comes out of it. Schosinsky (2007) proposes that the input is infiltration and the outflows are the evapotranspiration and the discharge to the aquifers. The simplified system is shown in **Figure 8**.

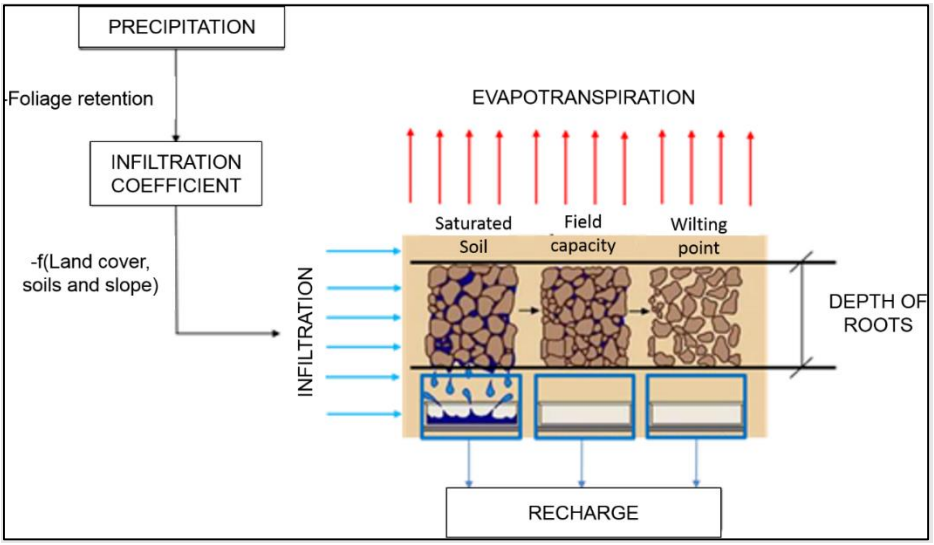

Figure 8. Idealized model for calculating recharge. Modified from *(Schosinsky N, (2007))*.

3.4. Hydrochemistry analysis

The chemical data of the Dabeiba thermal waters obtained from the National Inventory of Hot Springs (2012) by the SGC and the compiled dataset realized by (Gómez , 2019) are showed in **Table 2**.
(See Annex_01_GDB_MontoyaParra/06_Procesamiento/00_Tablas_Informe).

The analytical techniques used were standard methods such as volumetric analysis, ion chromatography, UV spectrometry, atomic absorption, inductively coupled plasma techniques, and Off-Axis ICOS (Integrated Cavity Output Spectroscopy) high resolution absorption laser spectroscopy for isotopes. The major chemical constituents were analyzed in the Water and Gas laboratory and the Stable Isotope Laboratory from SGC (Gómez , 2019). The cations using an average multiyear data were Na^{+}, K^{+}, Ca^{+2}, Mg^{2+}, Li^{+} and Sr^{2+} while the anions were HCO_3^{-}, F^{-}, SO_4^{2-} and Cl^{-}.

Table 2. Major chemical constituents, pH and the temperature of thermal waters from Dabeiba. The species of the solution in Mg/L. Modified from *(Gómez , 2019)*.

Sample	T (°C)	pH	Li	Na	K	Ca	Mg	SiO2	B	Cl	SO4	HCO3	TDS
Mohán (Mh)	30,00	7,39	7,52	4029,25	118,52	23,63	22,73	122,89	84,20	3446,23	2469,00	1439,80	12444,00
Chobar (Ch)	28,40	7,84	2,07	3122,00	41,30	30,70	23,50	84,49	71,07	4405,00	725,90	1751,00	8984,00
Guineales (Gui)	26,10	7,97	1,36	3332,00	40,00	24,00	18,44	27,04	75,03	5072,47	636,00	1415,20	9480,00

Initially, the charge balance error (CBE) was calculated for all springs to verify the reliability of the chemical data set obtained by the SGC in order to avoid analyzing a sample with ionic imbalances (Gómez , 2019). If CBE exceeds +/- 10%, the sample is not suitable for plots and geothermometers (Nicholson, 1993).

The Cl-SO4-HCO3 diagram is used to characterize the type of water in order to classify and associate the geothermal fluids with the geology and the subsurface process. The diagram of CL-Li-B and Cl-Sr-B was generated using "conservative" elements. In this case, (Gómez , 2019) detected that lithium in this case is regarded as a "conservative" element because in high temperatures it is highly mobile, despite being reactive. And the B is also regarded as conservative because in a geothermal system it only forms as a soluble mineral and their sources of supply to the geothermal fluid are too limited to be saturated with any mineral

(Arnórsson, 2000). Following this, the Na-K-Mg diagram proposed by Giggenbach (1988) was applied to establish the physicochemical balance between the fluid and the host rock, given a first sight of the temperature of the reservoir and identifying if they are suitable for the solute geothermometers. All the diagrams and the calculation of solute geothermometers were performed and adapted from Gomez, (2019), based on the spreadsheet by (Powell & Cumming, 2010). The methodological development is shown in a summarized way in ***Figure 9***.

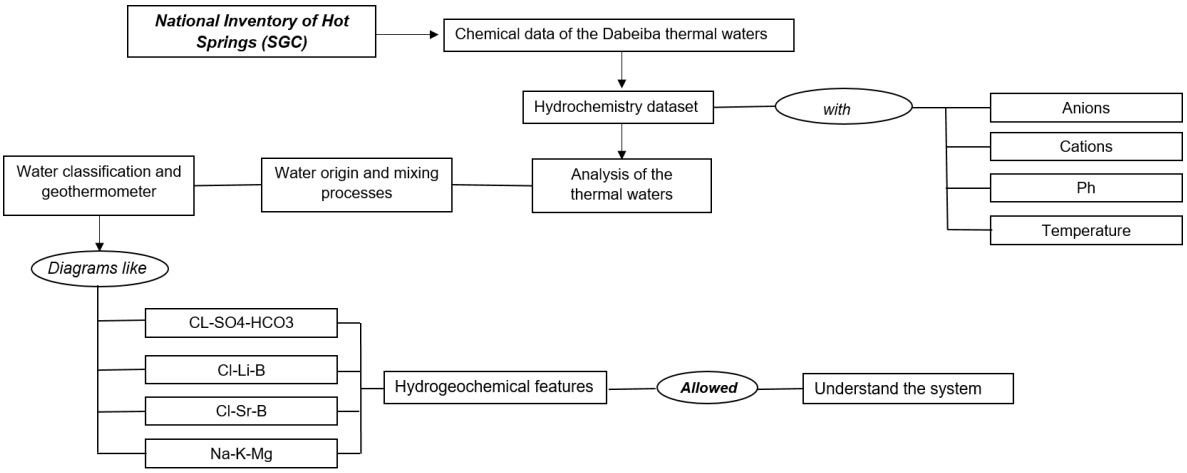

Figure 9. Methodological flowchart of the hydro geochemistry. Adapted from *(Gómez , 2019)*.

3.5. Low temperature thermochronology

Apatite (AHe) and zircon (ZHe) helium dating is a widely applied thermochronometric technique. Assuming a cooling rate of 10 °C/Myr, ^{4}It completely diffuses out of the apatite crystal at temperatures above 80 °C, it is completely retained below 40 °C, and partially retained between 40° and 80 °C (termed the partial retention zone (PRZ) (Wolf et al., 1998). Likewise, for zircon, assuming a cooling rate of 10 °C/m.y., ^{4}It is retained at temperatures below ~140 °C, and completely lost above 200 °C (Reiners et al., 2002, 2004). In this research we primarily focused on the AHe dataset, as the thermal sensitivity of the apatite system is lower and it is sensitive to processes in the uppermost ~1–3 km of the crust, assuming a mean annual surface temperature of 10 ± 5 °C and a geothermal gradient of 25 °C/km (Stockli, 2005). The low-temperature sensitivity of the AHe thermochronometer allows the assessment of small-scaled heating and cooling events related to tectonic, structural, erosional, and hydrothermal processes (Farley and Stockli, 2002; Ehlers and

Farley, 2003; Stockli, 2005). For the specific case of the geothermal studies in extensional geothermal plays, the (U–Th)/He thermochronometry has been applied to address the timing and rate of footwall exhumation and to assess the pre-extensional thermal state of the crust (Stockli, 2005, and references within).

4. RESULTS

4.1. Thematic maps

The calculation of the potential recharge model adapted from (Schosinsky N, (2007)), requires a series of physic variables: land cover and soil types, geology and structural patterns, precipitation, evapotranspiration, temperature and runoff. The four variables that depend on the physical components of the area are shown in ***Figure 10***.

4.1.1. Land Covers

Land cover types represent the way in which the recharge process is affected by land usage. To the West of the study area, forest is the most predominant land cover, with a patch of agricultural zones and homogenous vegetation. To the east, the pastures and open areas increase (See Annex_01_GDB_MontoyaParra/06_MXD/Landscover_1:80.000). The spatial distribution of the land covers indicates that 140.000 hectares are Forests, representing the 51% of the area. On the other hand, the agricultural covers represent the 27% of the the area, with approximately 72.500 hectares. The pastures have an approximate extension of 37.000 hectares, representing 14% of the spatial distribution in the study area. The remaining 8% is made up of urban areas, areas without vegetation, inland waters, areas of low vegetation and permanent crops, the latter being the most representative in the remaining distribution.

4.1.2. Soil types

Soil type were classified by Instituto Geográfico Agustín Codazzi (IGAC, 2007) in a scale of 1:50.000. These maps reflect the granulometry of the first centimeters of soil and it is represented in eight main texture types, from sandy to clay, franc being the most far extending, followed by silt, sandy, and finally areas of high clay content. The predominantly sandy texture is observed in a smaller proportion to the North of the study area (See Annex_01_GDB_MontoyaParra/03_MXD/Soil_Types_1:80.000). The spatial distribution of the soil texture indicates that 106.000 hectares have a sandy loam to clay texture representing 39% of the study area. Sandy to clayey textures also occupy the 31% of the

study area with 83.000 hectares. Other representative soil texture is clayey that represents the 22% of the area with 59.000 hectares.

4.1.3. Geology

From the hydrogeological perspective, each lithological unit has its own characteristics that can facilitate infiltration or generate runoff. The Penderisco Formation rocks, the basalts of the Botón, the diabases of San Jose de Urama are the lithologies with the higher degree of compaction. In turn, they generate more rugged reliefs, which greatly favor the generation of surface drains. The most representative lithology in the study areas is The Urrao Member of the Penderisco Formation Cañasgrodas (The Urrao member) (K2alu). This lithology represents the 27% with 73.000 hectares. Other formation with a lot of importance is Santa Cecilia La Equix that occupies 50.000 hectares, representing 19% of the area. On the other hand, 16% of the study the area (42.000 hectares) does not have geological cartography information.

It is important to highlight that the drainage area is formed by a complex volcanic-sedimentary rock of different ages, separated by regional structures associated to the Dabeiba Pueblo Rico Suture Zone (DPSZ). This zone overlaps into the lithology a preferential direction of subsurface and groundwater flow.

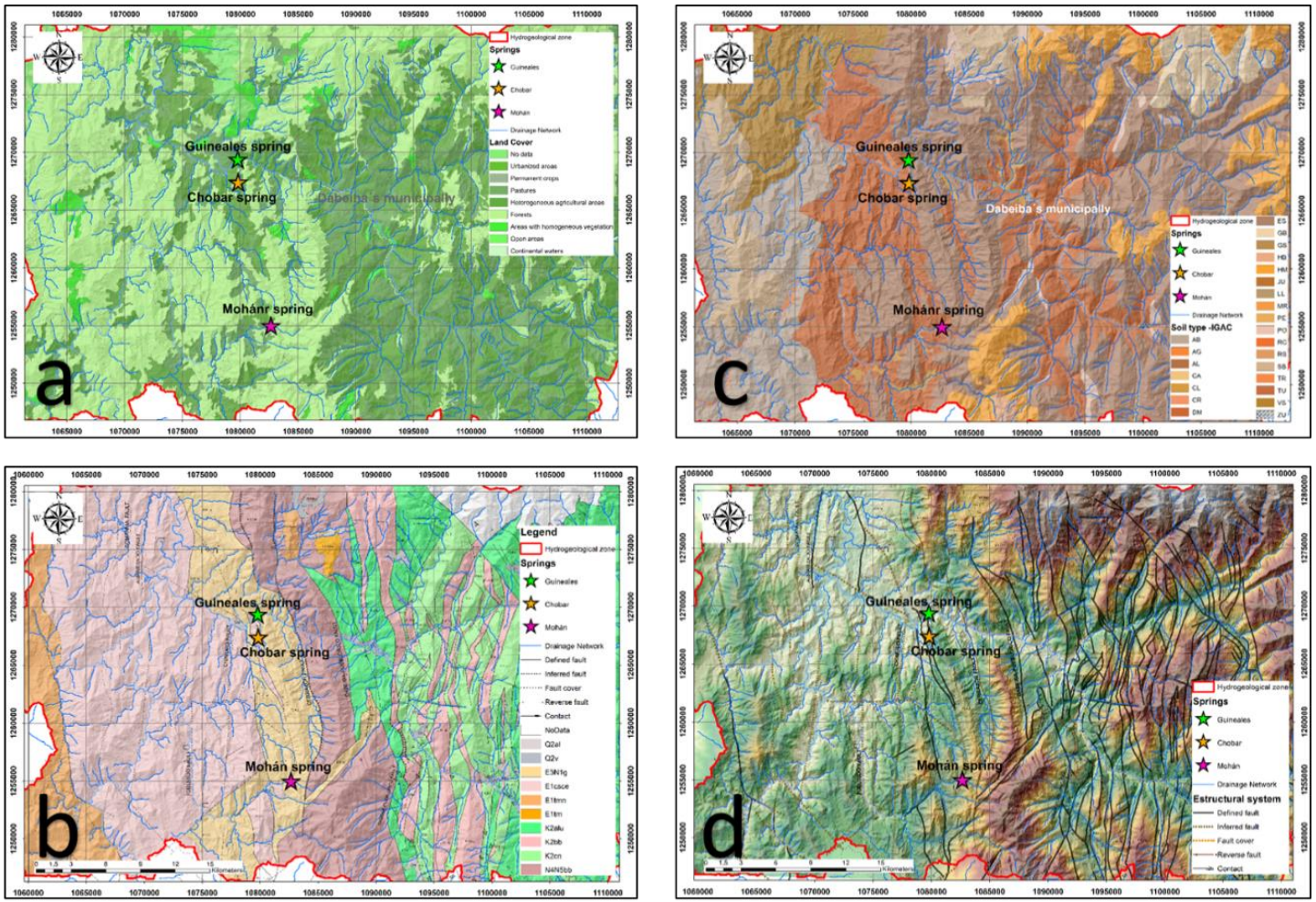

Figure 10. Thematic maps with physical conditions. a). Land covers, adapted from *(CORINE LAND COVER, 2010)*. b). Geological units, adapted from *(Rodriguez, Zapata, & Gomez, 2012)*. C). Soil types, adapted from *(IGAC, 2007)*. d). Structural patterns, adapted from *(Botero G, 2018)*.

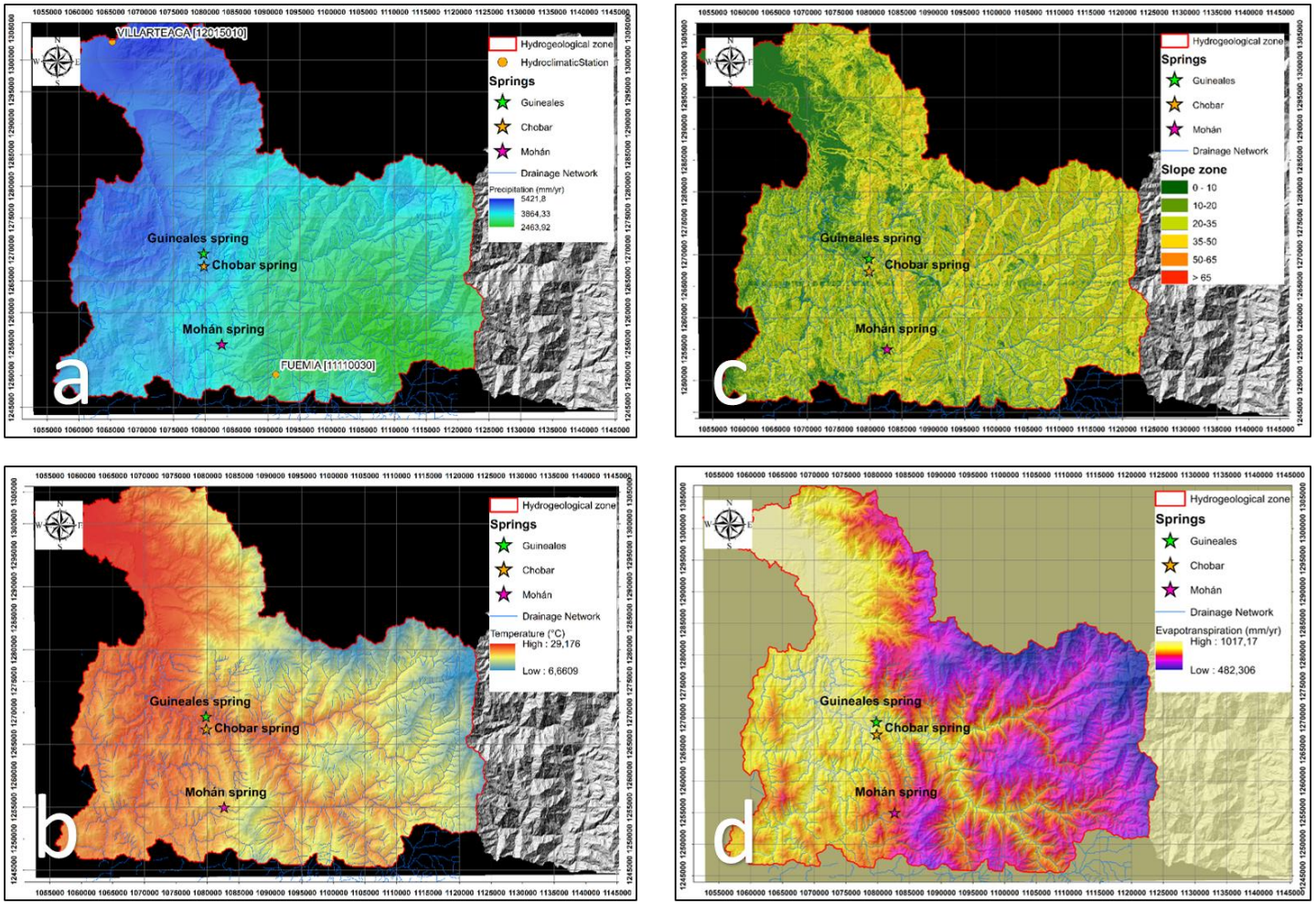

Figure 11. Thematic maps with climatological variables. a) Spatial distribution of precipitation, generated with a national deriva, proposed by Alvarez, 2007; b) Spatial distribution of mean temperature. c) Spatial distribution of slopes, generated in degrees; d) Potential evapotranspiration distribution, generated with Cenicafe´s equation.

4.1.4. Precipitation

The necessary climatic variables for modeling are precipitation and evapotranspiration in millimeters per year, and the average monthly temperature. Their spatial distribution is shown in **Figure 11**. The average multiannual precipitation was calculated from two stations that had daily rainfall records and used to find the multi-year average monthly cycle for 35 years of data. Due to the lack of data necessary to generate a direct interpolation of the values recorded in the stations, the approximate behavior of the rain was deduced from the rainfall map generated by (Álvarez V., 2007) for the whole country. We decided to apply a local correction of the magnitudes registered at the stations Since there were not enough stations to perform a direct interpolation, a local correction was made to the regional drift based on the data from the two stations. The values vary from 2200 mm/year towards the South, reaching up to 5420 mm/year towards the area near the Antioquia Urabá.
(See Annex_01_GDB_MontoyaParra/03_MXD/Precipitation_1:140.000).

4.1.5. Temperature and potential evapotranspiration

The distribution of potential evapotranspiration and temperature were calculated with empirical relationships that depend on elevation with respect to sea level. However, the model included evapotranspiration series calculated from data of the meteorological stations and approximated to the model following the Thornthwaite equation. (See Annex_01_GDB_MontoyaParra/03_MXD/Evapotranspiratation_1:140.000).

$$ETP = 1{,}6\left(10\frac{T}{I}\right)^{a}$$ ***Equation 2***

Where ETP is the potential evapotranspiration, T (in °C) is average monthly temperature, and s the annual caloric index given by:

$$I = 12\left(\left(\frac{T_{anual}}{5}\right)^{1.514}\right)$$ ***Equation 3***

And the exponent *a* is given according to the following equation:

$$a = \left(675*10^{-9}\right)I^{3} - \left(771*10^{-7}\right)I^{2} + \left(179*10^{-4}\right)I + 0{,}492$$ ***Equation 4***

4.2. Preferential directions

The channels and alignments of the water currents are usually controlled by the present geological structures (faults and fractures) (Flórez, Ramírez , & Monsalve, 2012). In order to know with certainty the general trends in the orientation of these channels, it was necessary to do a statistical analysis of the different sections at the drain network and the lengths of persistence. The analyses of each lithology are showing four preferential directions (**Figure 12**).

The Santa Cecilia-La Equis complex *(E1csc denotation)* and the Mandé Batholith have the same structural control marked by the L1, the same direction is marked to the center of this area. The eastern portion of the area, represented by the Nutibara Member *(K2cn denotation)*, the Barroso formation *(K2bb Formation)*, and the Urrao Member of the Cañasgordas Complex *(K2aluFormation),* has a common structural control marked by the L1 direction.

The intrusive bodies located to the West *(N4n5b Formation and E1tmn formation)* have two structural controls marked by the drainage direction, L2: 067° and L3:112°. ***Figure 13*** indicates that orientations L2 and L3 do not have any relation with the lineaments present in this section of the study area (157° and 130°). Finally, the Guineales Formation *(E3n1g denotation),* shows a structural control marked by the drainage with orientation of L4: 340, coincident with the lineaments present in the study area (orientation 340).

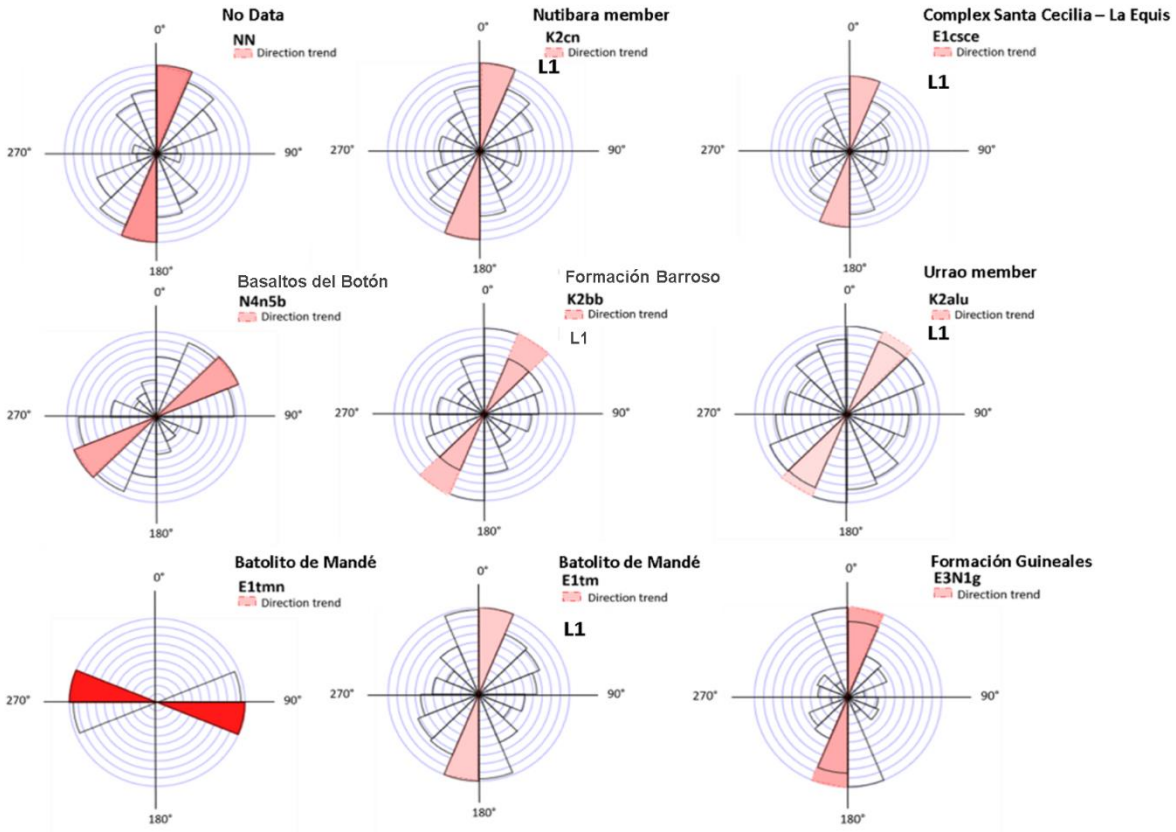

Figure 12. Preferential directions of drainage network for each lithology. Generated from *(Arken.nmbu.no/qgisplugins, 2019)*.

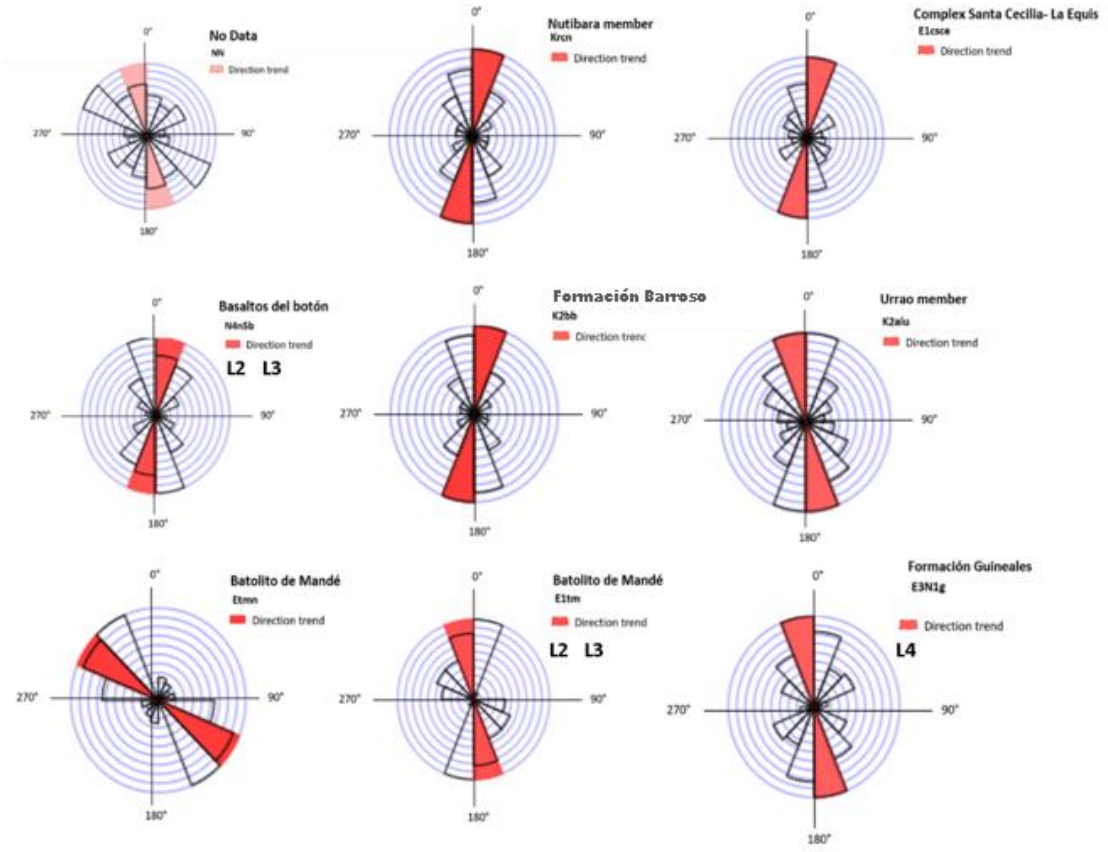

Figure 13. Preferential directions of faults and lineaments for each lithology. Generated from (Arken.nmbu.no/qgisplugins, 2019).

The general tendency of the drainage-network and lineaments ***Figure 14*** is showing a strong correlation between both components, and the regional orientation of the different units (See Annex_01_GDB_MontoyaParra/06_MXD/Procesamiento/03AnlisisEstructural). According with our data, the preferential direction in the study area varies between L1 to L2 (010° and 045°).

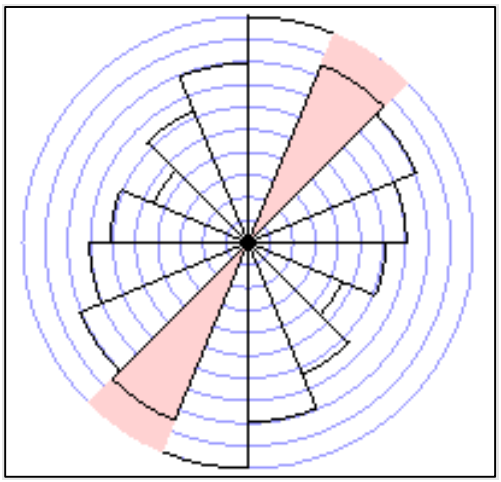

Figure 14. General tendency of drainage network and lineaments in study area. Generated from *(Arken.nmbu.no/qgisplugins, 2019)*.

4.3. Hydrogeological properties of study area (Recharge zones)

It should be noted that the recharge estimated by the methods of soil moisture balance and flow simulation in the unsaturated zone is considered potential. It is based on surface hydrological data and an approach to the unsaturated area, but it does not directly consider hydrogeological information (groundwater levels), therefore, such recharge may or may not reach the water table. However, this analytic tool under the approach presented tries to associate the behavior of the recharge with the spatial factors that control the infiltration, without detailing the magnitude largely.

4.3.1. Potential recharge model (hydrometeorological soil´s balance)

The potential recharge model was calculated from a semi-distributed model developed in 2006 by Schosinsky and applied on a monthly scale. The model was based on the mass balance equation inside of the basin and required capturing the spatial distribution of the recharge, identifying areas with homogeneous characteristics from overlapping soils and coverages (Bastidas & Vélez O, 2018).

The model uses the amount of precipitation distributed in an area and determining the amount of water that infiltrates and accumulates in the pores of the soil to bring it to field capacity, which is the maximum water capacity that can hold a soil not saturated. Subsequently, the process of evapotranspiration is quantified and if the amount of infiltration is enough to bring the soil to field capacity and satisfy the need for evapotranspiration, the surplus of the water that infiltrates, percolates to recharge the aquifer.

4.3.2. Parameters and simulation periods

The potential annual recharge was estimated for three periods with different hydrological conditions: normal condition (2014), dry year (1986) and wet year (2010). This classification was made based on the historical records of two IDEAM stations; FUEMIA, representing the average distribution of the center towards the South of the zone, and VILLARTEAGA, showing the behavior of the center and North of the zone (See Annex_01_GDB_MontoyaParra/06_Procesamiento/01_Recarga/SeriesIdeam/01_Precipitacion). These average annual rainfall data were constructed considering the daily values reconstructed at an average annual cycle (**Table 3**). Each annual period starts in the month of May given that, according to the annual rainy cycle, in the following month (June) (**Figure 15**) the maximum precipitation occurs, so we can assume that the soil lacks initial humidity.

Table 3. Summarized simulation periods based in FUEMIA station and VILLARTEAGA station.

Station	*Condition*	*Period*	*Precipitation [mm/yr]*
VILLARTEAGA	Normal year	2014	5815.8
	Dry year	1986	4281.9
	Wet year	2010	6794.6
FUEMIA	Normal year	2014	1403
	Dry year	1986	1185
	Wet year	2010	1557

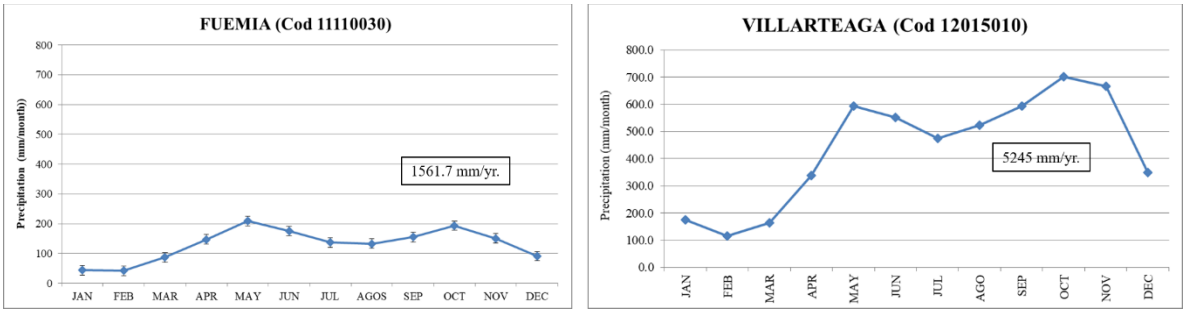

Figure 15. Annual rainfall cycle for the two base stations. On the left, FUEMIA with a multiannual average of 1561 mm/year; on the right VILLARTEAGA with a multiannual average of 5245 mm/year.

The model requires the monthly series of potential evapotranspiration (ETP) for each year of simulation. Given the high percentage of missing stations, an empirical evapotranspiration estimation method was used. Potential evapotranspiration was calculated based on the method proposed by Thornthwaite (See

Annex_01_GDB_MontoyaParra/06_Procesamiento/01_Recarga/SeriesIdeam/02_Temperatura/CalculoEavapotranspiración) which calculates the ETP as a function of temperature.

Table 4. Summarized simulation periods of evapotranspiration based in MUSINGA station and VILLARTEAGA station.

Station	***Condition***	***Period***	***Evapotranspiration [mm/yr.]***
VILLARTEAGA	Normal year	Average	1043.1
MUSINGA	Normal year	Average	1349.9

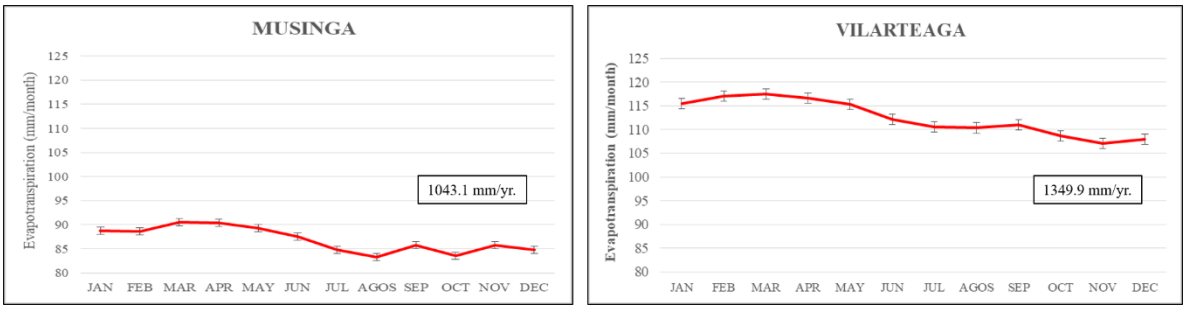

Figure 16. Annual evapotranspiration cycle for the two base stations. On the left, MUSINGA with a multiannual average of 1043.1 mm/year; on the right VILLARTEAGA with a multiannual average of 1349.9 mm/year.

4.3.3. Potential zones mapping

Direct annual potential recharge maps were obtained for each of the three scenarios studied, where an approximation to the spatial distribution of recharge due to precipitation in the area is observed. **Figure 17** shows the spatial distribution of the recharge zones for a normal year, varying in a range between 0 and 3093 mm/year. This range increased its maximum value for one year in humid conditions, where it reached 3950 mm/year to the North mainly, and decreased in dry conditions where maximum recharge of 2190 mm/year was obtained, as shown in **Figure 18**. In total, 281 zones of homogeneous characteristics were generated, and the magnitude of the recharge was calculated to understand its spatial distribution.

(SeeAnnex_01_GDB_MontoyaParra/06_Procesamiento/01_Recarga/ZonasHomogeneas/Zonas_Variable/ZonasHomogeneas).

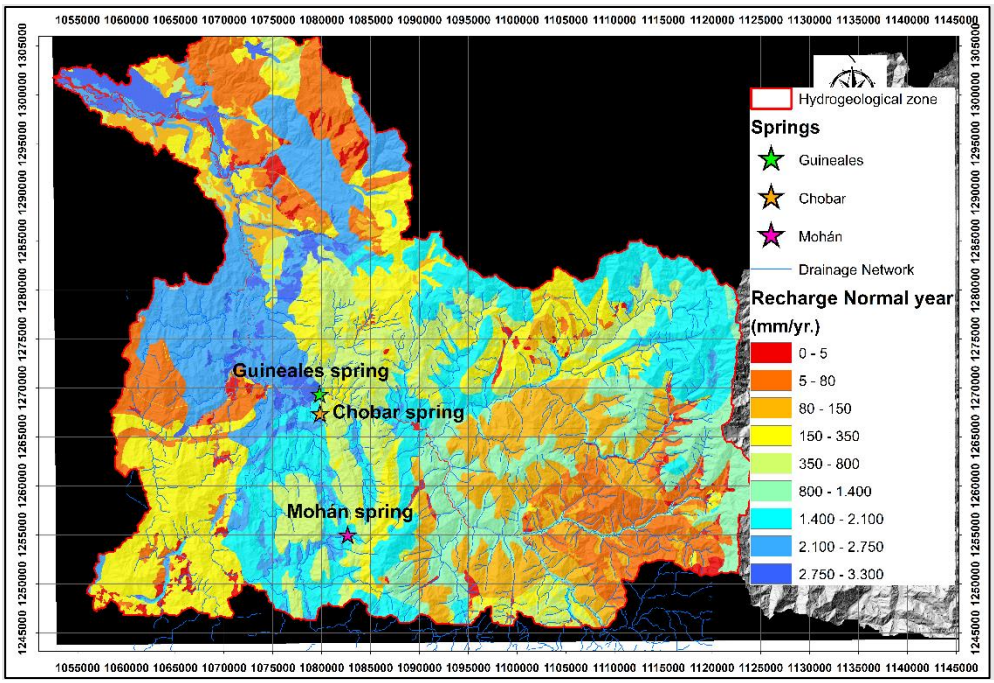

Figure 17. Spatial distribution of the potential recharge by precipitation for a normal year.

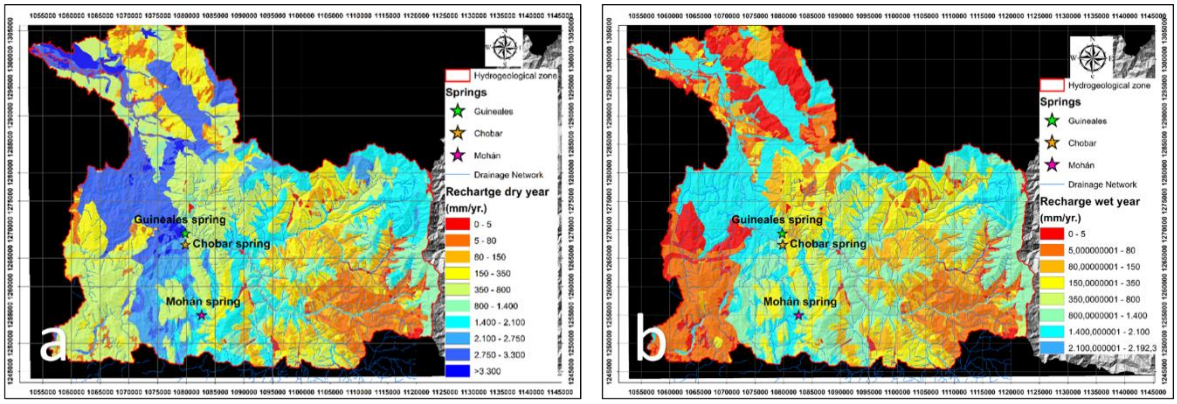

Figure 18. Spatial distribution of the potential recharge by precipitation. a) Potential recharge for dry year; b) Potential recharge for dry year.

As a joint analysis, there is a temporal variability of recharge as a direct response to climatic conditions, especially precipitation. However, several predominant ranges are observed between 5 and 350 mm/year and, which remain constant both in the spatial distribution and in time.

On the other hand, the areas of highest recharge in the three conditions are observed mainly towards the North and West of the hydro-climatic zone, adding to small areas considered as accumulation due to the steep slope changes in the surrounding areas that favor the accumulation of runoff and subsequent infiltration. These zones coincide in the center of the

zone, surrounding the hydrothermal sources of interest, temporarily varying only in small orders of magnitude. (calculation files_See Annex_01_GDB_MontoyaParra/06_Procesamiento/01_Recarga/ZonasHomogeneas/ModeloCalculo).

5. DISCUSSION: GEOTHERMAL CONCEPT MODEL

5.1. Hydrochemistry

As thermal fluids move away from the upwelling zone along a fault zone, they mix with cooler groundwater or meteoric water, as indicated by an increase of bicarbonate and magnesium and decrease of boron, sulfate and chloride (Moeck, 2014). The DGS are sodium-chloride slightly diluted waters close to mature water (**Figure 19**), generally associated with the opening of discontinuities that allow fluid circulation. The rupture lines generated by the structural system also allowed the meteoric water to be filtered at greater depths, picking up the heat of the system (Kresic & Stevanovic, 2010).

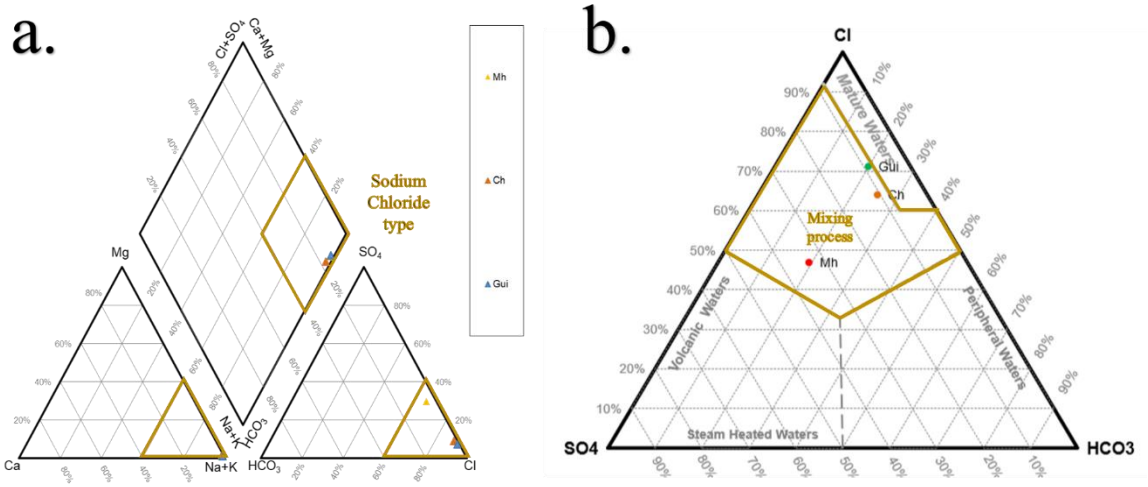

Figure 19. Piper diagram of Dabeiba hot springs. Sodium Chloride type. Mohan spring is represented by an orange dot, Guineales by a blue dot and Chobar by a brown dot.

The Stiff diagrams show a clear ion-exchange of the sources, supporting the chlorinated sodium compositional classification in the three cases and showing in turn a decrease in the CL anion as it advances towards the South, increasing the concentration of SO4 in the spring of Mohán and notoriously increasing the electrical conductivity as shown in **Figure 20**. (See Annex_01_GDB_MontoyaParra/03_MXD/StiffDistribution)

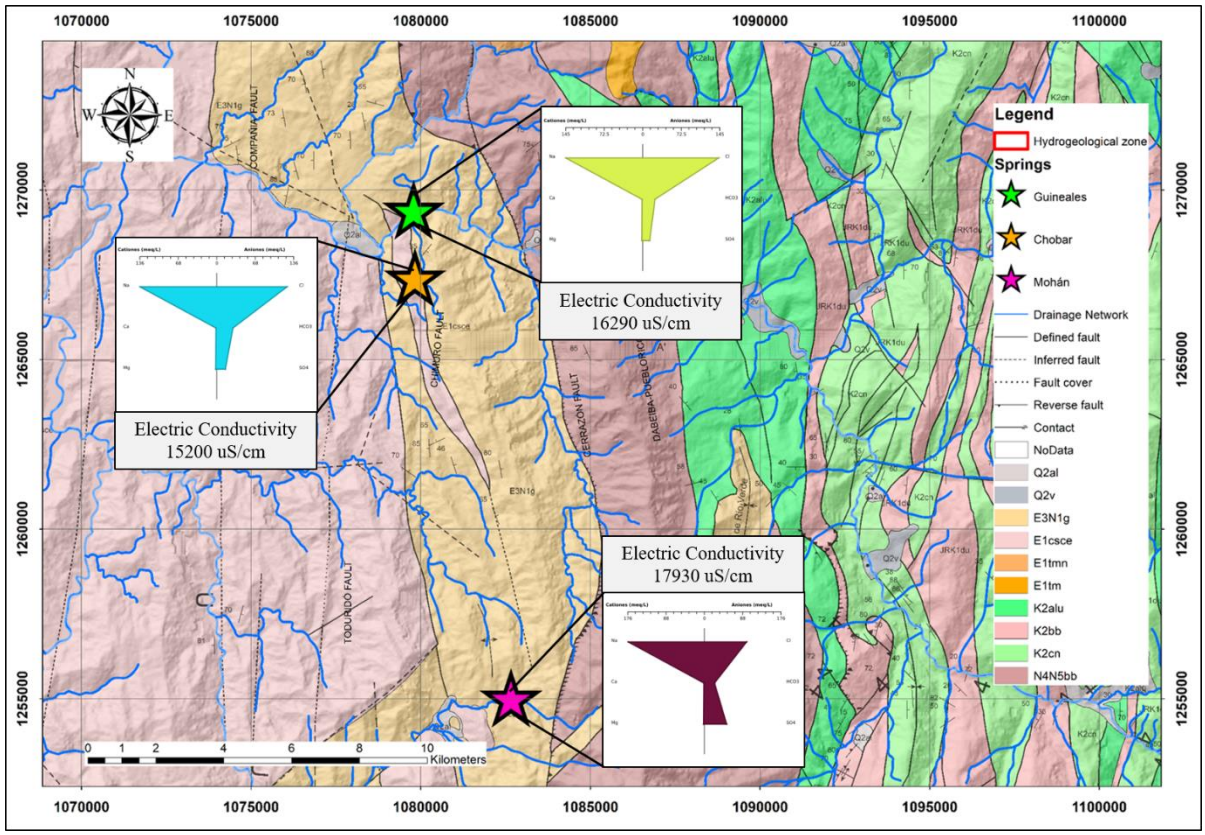

Figure 20. Stiff´s diagrams of Dabeiba springs. Spatial distribution in geological map. The green diagram represent Guineales spring, the blue diagram represent Chobar spring and the violet diagram represent Mohán spring.

We expected that the water in the study zone could be mixed with meteoric waters or groundwater. It was expected that mixing processes with meteorological water or underground reserves could be generated in the study area; in order to verify this evaluation processes were conducted. Is possible that due to the mixing process, the water emerging on the surface may have been cooled down when the fluid ascended from the cold groundwater reservoir, and this process could have disturbed the chemical equilibrium.

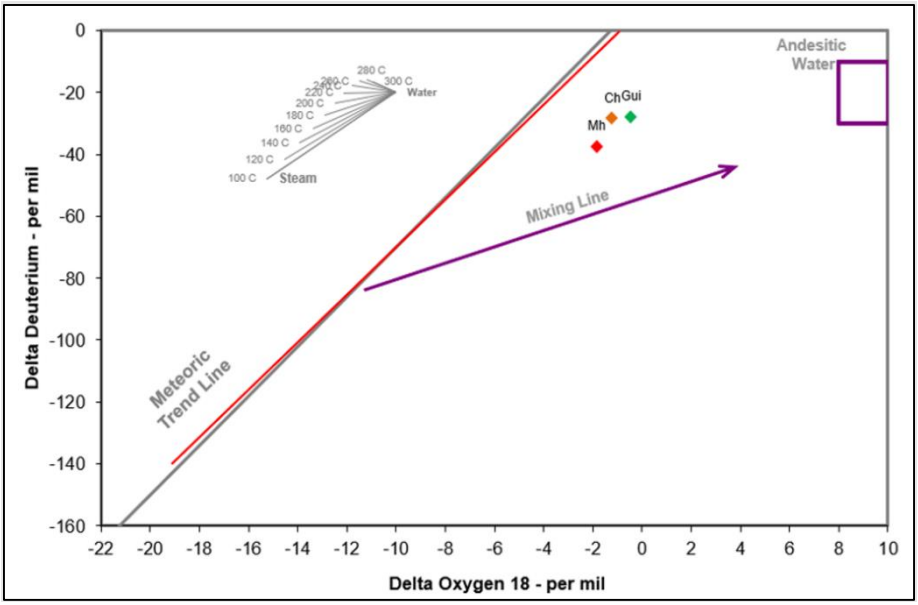

Figure 21. Cross-plot of the stable isotopes of water (δ18O – δD). The red line is the segment of the Colombian Meteoric Line (CML) and the gray line is Global Meteoric Water line GWML, the range of andesitic water as proposed by Giggenbach (1992). Dabeiba springs dots reflect a slight rise and to right. Mohan spring is represented by a red dot, Guineales by a green dot and Chobar by an orange dot. Adapted from *(Gómez , 2019)*.

Figure 21 shows that the thermal waters of the DGS are plotting to the right of the GWML (Global Meteoric Water Line) and CML (Colombia Meteoric Line) with a slight slope. This result may indicate that the thermal waters have been influenced for slightly mixing, probably for ground waters with magmatic waters, or fossil waters trapped in marine sediments (Gómez , 2019). During the mixing process, water-rock interaction might generate an exchange of oxygen between geothermal waters and rock if the temperature is ≥ 220°C, where the percentage of oxygen-depleted from the rock is equal to the enrichment of oxygen in the geothermal water (Chandrasekharam & Bundschuh, 2008).

The sodium-chloride waters are related to a geothermal system where they ascend through the reservoir as a single-phase fluid until they reach a depth where they boil and the CO2 and H2S gases are dissolved in the fluid phase, and travel in the vapor phase that allows the ascent of these ions (Browne & Rodgers , 2006). These springs could be related directly to the deep reservoir with minimal mixing effects or with up flow zones in high temperature systems. To complete the analyses, the plot of conservative elements (Cl, Li, Sr and B) was used to determine if the springs come from the same system. This plot is shown in ***Figure 22***.

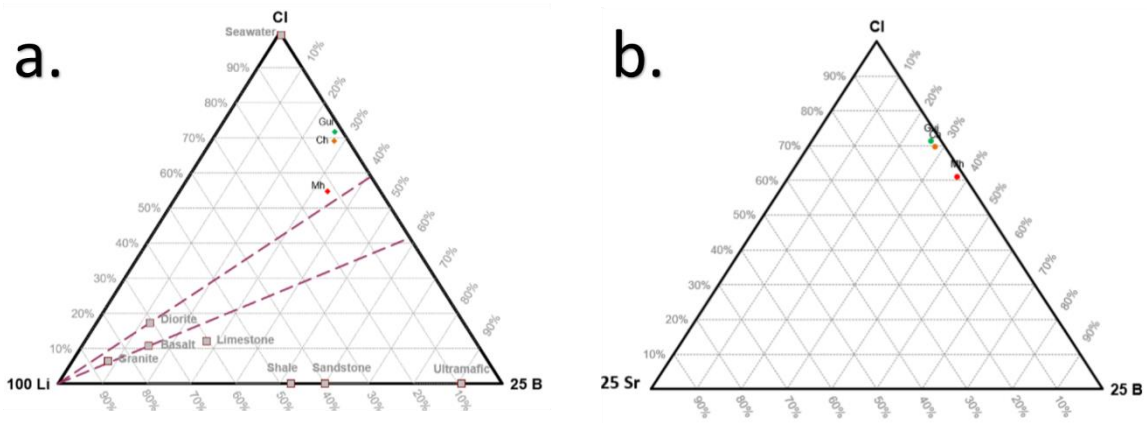

Figure 22. Plot of conservative elements proposed by Giggenbach (1991). a.) Cl-Li-B Plot; b.) Cl-Sr-B Plot. In two cases Mohan spring is represented by a red dot, Guineales by a green dot and Chobar by an orange dot. Modified by (Gómez , 2019). The plots were made on using the spreadsheet of Liquid Analysis v3 (Powell & Cumming, 2010).

The second one is a ternary plot Cl, Sr and B where the Li is replaced by Sr, which is another conservative element present in these waters. Both ternary plots show a strong relationship between of Guineales and Chobar waters. On the other hand the high amount of B may suggest that the fluids travel rapidly to the surface probably because they do not have time to become incorporated into low-rank alteration such as clays and zeolites (O´Brien, 2010). Mohan is the only spring that is close to sulphate waters despite being from the same apex.

The Na-K-Mg diagram (Figure 23) shows that all the springs fall into the range of partial equilibrium, which is around 110°C for Guineales and Chobar approximately 150°C for Mohan spring. The diluted waters with a moderate concentration of HCO3 are influenced for the mixing process. They mixing development are still regarding to be used for certain solute geothermometry since they are falling in partial equilibrium, even with geothermometry is not possible the spatial distribution of the springs is an important tool to help with understanding the system (Nicholson , 1993).

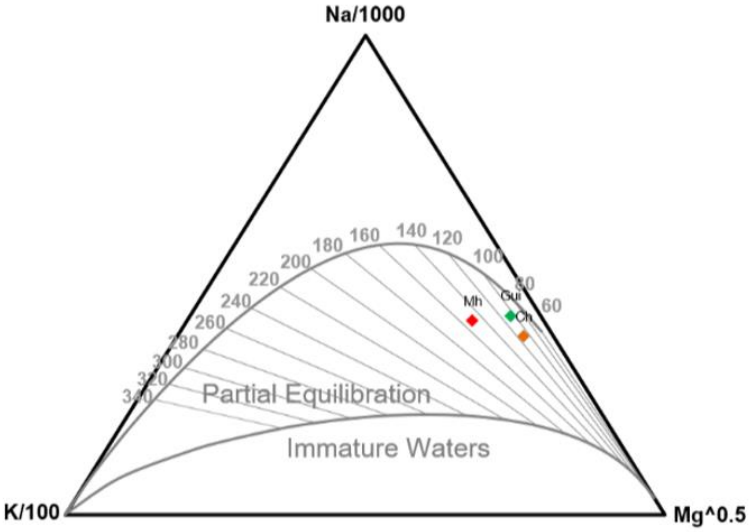

Figure 23. Na-K-Mg plot, adapted from *(Gómez , 2019)*. Mohan spring is represented by a red dot, Guineales by a green dot and Chobar by an orange dot. The plots were made on using the spreadsheet of Liquid Analysis v3 *(Powell & Cumming, 2010)*.

The silica geothermometers chosen are shown in the **Table 5**. Using the geothermometer of chalcedony, the maximum temperature calculated is 120°C in the Mohan spring, while the lowest one is 44°C at the Guineales spring. The Na-K-Ca geothermometer indicates a reservoir temperature around 125-170°C. However, this geothermometer in low temperature environments (<100-120°C), and/or with fluids relatively rich in CO2 or Mg may throw misleading temperature (Nicholson , 1993). The Na/K geothermometer indicates a reservoir temperature between 106 and 150°C, contrary to the calculation of K/Mg generated by (Gómez , 2019), which shows values below 122°C, with Mohan being the highest in all geothermometers.

Table 5. Reservoir temperatures (°C) estimated by solute geothermometers in the DGS, modified from *(Gómez , 2019)*.

Samples	*Chalcedony fournie & Potter, 1982*	*Na-K-Ca Fournier and truesdell, 1973*	*Na/K Giggenbach, 1988*	*K/Mg Giggenbach, 1988*
Mohan	124	170	150	122
Chobar	100	127	110	92
Guineales	44	125	106	94

The DGS can be characterized as a mixture of water in low portions with geochemical associations of the thermal sources as slightly diluted chloride waters. The "conservative" elements allowed to identify that the springs come from the same reservoir and the solute geothermometers reveal a temperature around 120-130°C that indicates a low enthalpy

system as it was proposed by Gómez (2019). (See Annex_01_GDB_MontoyaParra/06_Procesamiento/02_Hidrogeoquimica).

5.2. Mixing model

The DGS is probably related to an extensional Miocene event that allows the Guineales Formation, followed by an emplacement event characterized by high angle normal faults where the fluid flow along faults is controlled by the state of stress in the reservoir rock. The flow of the ground waters could be associated to the fault system that have the direction 022, this system affects the Batholith of Mandé, the Nutibara Member (K2cn), Barroso formation (K2bb), and Urrao Member of Cañasgordas Complex (K2alu), all these formations have the same structural patterns in its drains. The Guineales Formation (E3n1g) show a structural control marked by the drainage with orientation 340 showing a relation with the orientation off the lineaments presents in the study area. This orientation match with the location of the three thermal water sources in the surface. This could be related to the way in which heat is given from the deep source to the thermal emanations.

The results obtained in the hydrogeochemical analysis allowed to identify mixing processes, a deep heat source, and different contaminant elements associated with adjacent recharge areas related with the hydrothermal vents. The recharge zones respond largely to strong changes in slope, the magnitude of rainfall and soil characteristics. These more favorable factors are induced by the presence of a complex fault system, on which areas of greater potential are located to the West and Northwest of the area, according to the location of the thermal sources. It is possible that in very high recharge areas large contributions to the sources are generated. The sources generate with a moderately high residence time in the underground environment and return to the surface through decompression processes along the same fault systems that favored its infiltration. The behavior of the system and its relationship with the surface variables is shown in **Figure 24**.

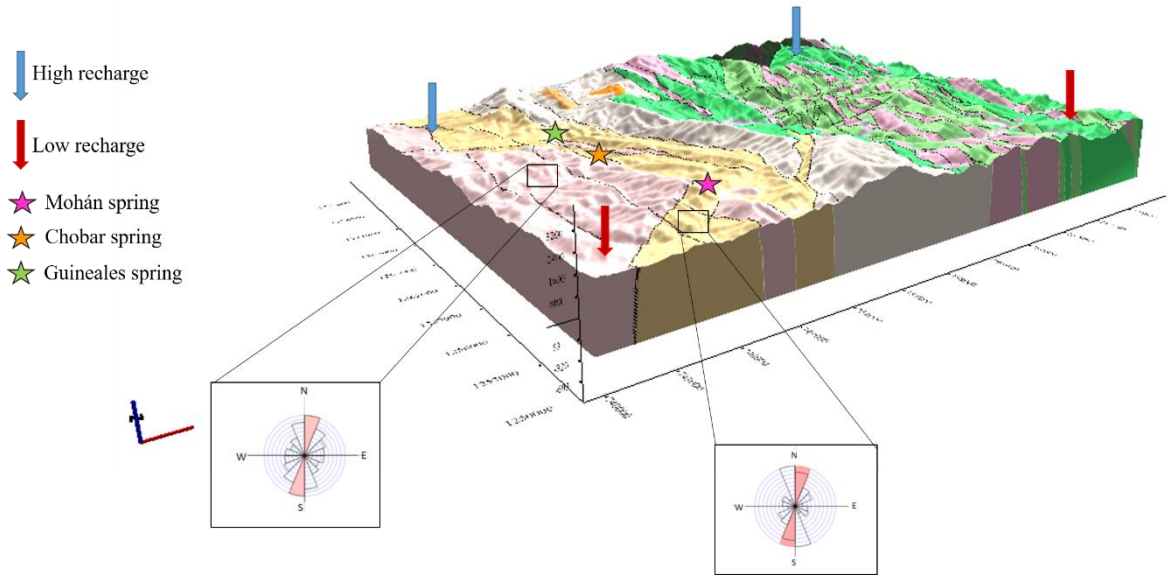

Figure 24. Geothermal conceptual model #1. Behavior of the surface system.

Hydrogeochemical characterization suggests that the Chobar and Guineales springs are in the margin of the system where they are more affected by the lateral flow, while Mohan spring is apparently more linked with the up flow. The concentration of CL, SO4, and B inferred that the system is influenced by a deep resource with a minimal diluted process and inferring that the system is interacting with degassing of magma of an intrusive, contributed by sedimentary layers or a process of water release from metamorphism of marine sediments.

5.3. Heat flow and advection

Cooling ages greatly enhance regional-scale exploration for blind geothermal resources. AHe thermochronometric data have been shown here to: 1) Estimate temperatures for hydrothermal fluids and (2) Identify zones of localized advection. AHe thermochronometry can be an accurate, easy, and cost-effective addition to standard regional-scale geothermal exploration practices. AHe data at the Guinerales Formation, located in the Chimuro Normal Fault hanging-wall, may has important implications on the utility of AHe thermochronometry to assess the long-term conductive equilibration, and the identification of hydrothermal fluid shows. We can see, that the hydrothermally reset AHe ages (1.7 - 2 Ma, Botero 2018)

correlates well with the temperature calculated from thermometry at the spring waters as shown in the previous section. The model-derived temperature estimates hydrothermal fluids (150 ±30°C °C). This implies that the zone distribution of completely reset and un-reset AHe ages and associated spikes represent the heterogeneity and juvenile nature of the hydrothermal fluids. The presence of reset AHe ages along the hanging wall range resulted from the interaction of hanging wall samples with hot (85°–135 °C) hydrothermal fluids, and provided some time constraints on the longevity of the DGS, whose lifespan is on the order of 0.1–2 Myr

However, the temperature of the geothermometers is below 150 ±30°C, being unattractive at first sight unlike other geothermal systems in the country. The understanding of the functioning of isotherms and the processes responsible for ascent depend largely on the genesis and evolution of the structural system. The DSZ may cause the geothermal gradient to rise around the Chimurró normal fault. Therefore, the complexity of geothermal systems of extensional type through the use of apatite AHe, permits us to join the thermochronology to the time, where the distribution and magnitude of advection in the foot and hanging wall, with subsequent redistribution of heat by hydrothermal fluids in the hanging wall located in the Guineales Formation as it has been proposed in several plays around the world (e.g. Gorynski K. , Walker, Stockli, & Sabin, 2014).

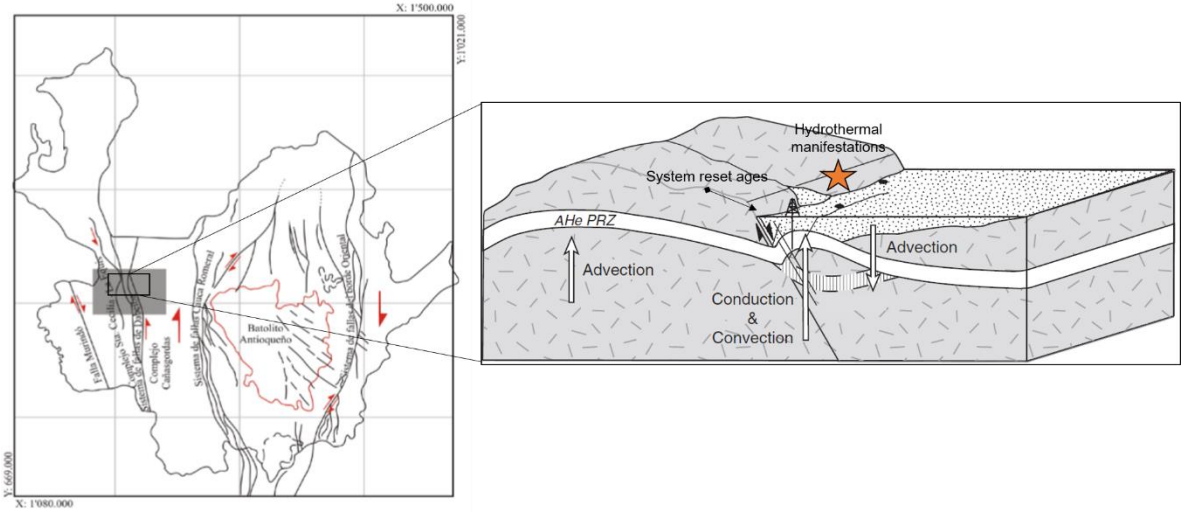

Figure 25. Block diagram adapted from Ehlers et al. (2001) and *(Gorynski K. , Walker, Stockli, & Sabin, 2014)*, showing the thermal characterization of normal faults where isotherms, represented here as the AHe partial retention zone (PRZ), are advected upward in rapidly exhumed footwalls of normal faults. Adjusted to structural system of Dabeiba.

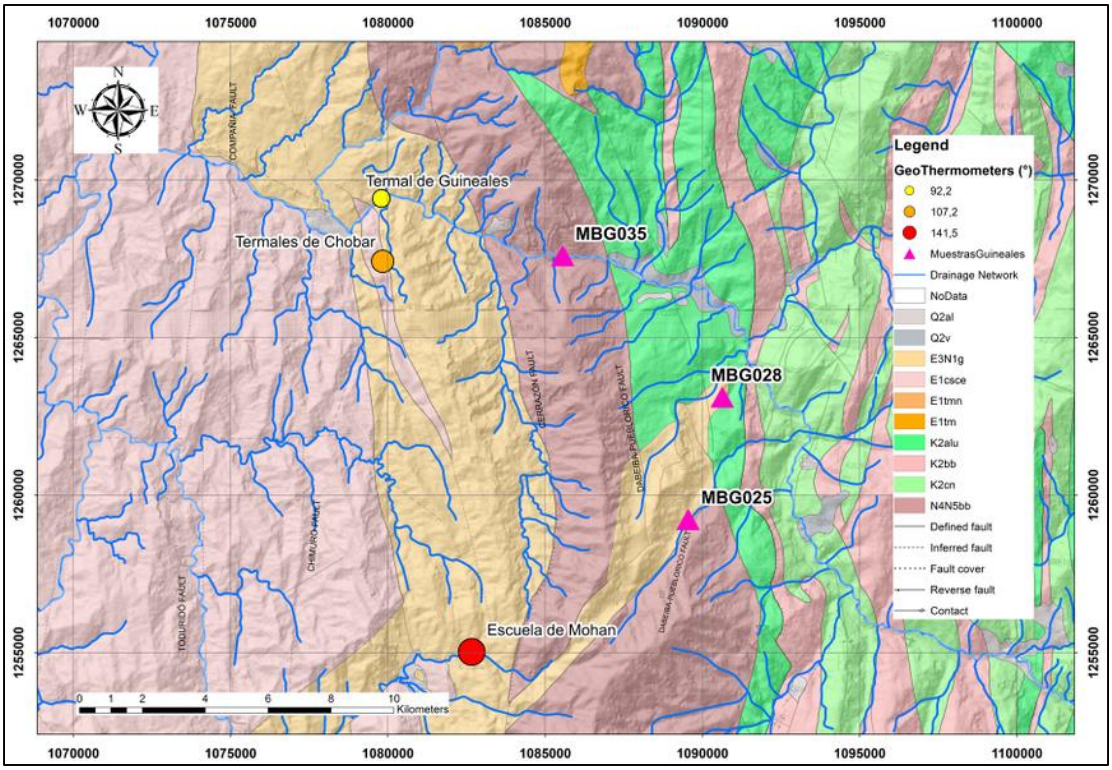

Figure 26. Geothermometers map and comparative samples with ages (U-Th)/He in apatite. The yellow dot represent Guineales spring; the orange dot represents Chobar spring; the red spring represent Mohan spring.

Finally, from the thermocronological data set (Botero G, 2018), it was possible to infer that the reverse fault system allowed the accumulation of the Guineales Formation, which apparently did not pass the zone of partial reset of ZHe. The ages of 1.7 M and 0 Ma seem to agree with a process of burial of the basin by the partial erase zone of Ap He, with current reset by the action of the advected upward in rapidly exhumed footwalls of normal faults, and the rise AHe partial retention zone (PRZ) and the isotherm to hit up the mixed fluids to the surface (Figure 25).

6. CONCLUSIONS

The reservoir is related to deep fracture zones in the meta-sedimentary rocks and cataclasites from the Guineales Formation. The seal rock is the impermeable Neogene sedimentary units from the same sedimentary formation and/or from an impermeable altered zone and a plutonic-metamorphic as the basement.

The suggested model for the DGS is related to a low enthalpy system formed by the isotherm advection in a local extensive system of the Chimuro Fault, along the Guineales Formation. The complexity of the DGS and the use of a multi-tool approach permitted us to join the thermochronology to the time, were the accumulation of the Guineales Formation, apparently did not pass the ZHe reset zone. The ages of 1.7 M and 0 Ma seems to agree with a process of burial of the basin by the partial erase zone of Ap He, with current reset by the action of the advected upward in rapidly exhumed footwalls of normal faults, and the rise AHe partial retention zone (PRZ). The isotherm allowed the thermal fluids to move away from the upwelling zone along the Chimuro fault zone, mixing with cooler groundwater or meteoric water, as it is indicated by an increase of bicarbonate and magnesium and decrease of boron, sulfate and chloride.

However, with new geothermal plant technologies, these controlled geothermal faults systems of medium temperature (150 ±30°C) could be developed at a small-scale. These geothermal programs could provide energy for small communities even in remote areas (Moeck, 2014). The suggested model for the Dabeiba area is summarized in **Figure 27**.

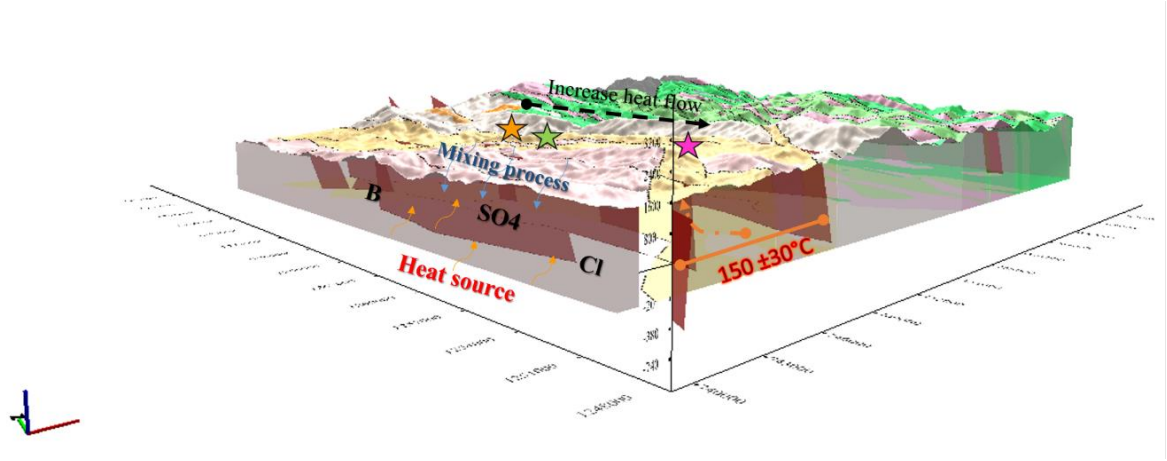

Figure 27. Geothermal conceptual model #2. Behavior of mixing process and heat source.

ACKNOWLEDGMENTS

The authors thank the different contributions made by the Engineer Manuela Botero and the work team of the National University of Colombia. To the company SHI S.A.S, for the time and resources implemented in the hydrogeological section of the article, especially to the engineer Breiner Dan Bastidas. To the geologist Adriana Londoño for her support in the compilation and organization of the databases. To EAFIT University, for logistical and administrative support during all years of academic training.

7. REFERENCES

Aguilera, P., García, Y., Martinez , G., Cruz, K., & Pacheco, M. (2017). *ANÁLISIS DE GASES DIFUSOS EN LA FUMAROLA AGUA SHUCA, CAMPO GEOTÉRMICO AHUACHAPÁN, EL SALVADOR.* Ahuachapán: LaGeo/Group CEL- Diplomado en Geotérmia.

Alcaldía del municipio de Dabeiba. (12 de 10 de 2018). *Dabeiba.gov-Sitio oficial* . Obtenido de Dabeiba.gov-Sitio oficial : http://www.dabeiba.gov.co/generalidades.html

Álvarez , E., & Gonzalez, H. (1978). *Geología y geoquímica del Cuadrángulo I–7 (Urrao). Mapa a escala 1:100.00.* Medellín: Ingeominas. Informe 1761. 347p.

Álvarez V., O. D. (2007). *Cuantificación de la incertidumbre en la estimación de campos hidrológicos. Aplicación al balance hidrológico de largo plazo.* Medellín: Postgrado en Aprovechamiento de Recursos Hidraúlicos-UNAL.

Álvarez, J. (1970). *Mapa geológico generalizado y localización del muestreo geoquímico de la Cordillera Occidental, departamentos de Chocó y Antioquia.* Medellín: INGEOMINAS- Memorias inéditas.

Arken.nmbu.no/qgisplugins. (20 de Febrero de 2019). Obtenido de Arken.nmbu.no: http://arken.nmbu.no/~havatv/gis/qgisplugins/LineDirectionHistogram/

Arnórsson, S. (2000). Mixing process in upflow zones and mixing models, Chapter 11. Isotopic and chemical techniques in geothermal exploration, development, and use. Sampling methods, data handling, interpretation. . *International Atomic Energy Agency. Vienna*, 152-199.

Bastidas, B. D., & Vélez O, M. V. (2018). *Estimación de la recarga potencial por precipitación del acuifero transfronterizo del Amazonas.* Medellín: Publicaciones Resechgate.

Botero G, M. (2018). *Proveniencia y estilo estructural de la Formación Penderisco y las sedimentitas de Beibaviejo: Relación con el bloque Panamá-Choco (PCB).* Medellín: Grupo de Estudios Tectónicos (GET)-Universidad Nacional De Colombia.

Browne , P., & Rodgers , K. (2006). Occurrence and significance of anomalous chloride waters at the Orakei Korako geothermal field, Taupo Volcanic Zone, New Zealand. *Geothermics 35(3)*, 211-220.

Calle , B., & Salinas, R. (1986). *Geología y geoquímica de la Plancha 165, Carmen de Atrato.* Medellín: INGEOMINAS-Informe de presentación. 140p.

Chandrasekharam, D., & Bundschuh, J. (2008). *Low-enthalpy geothermal resources for power generation.* Leiden: The Netherlands, CRC Press/Balkema. D'Amore, F., and Truesdell, AH-1985.

CORINE LAND COVER. (2010). *Mapa de coberturas del Departamento de Antioquia, Escala 1:100.000.* Medellín: SIG_Gobernación de Antioquia.

Diaz Cañas, J. S. (2015). *Marco bioestratigráfico y proveniencia de la Formación Penderisco, y su significado en la formación de un domo marginal a las Fallas de Romeral.* Bogotá: Universidad Nacional de Colombia. 56.

Duque-Caro, H. (1990). *The Choco Block in the northwestern corner of South America structural tectonostratigraphic and paleogeographic implications.* Bogotá.

Flórez, C., Ramírez , M., & Monsalve, G. (2012). *Metodología para el Tratamiento de Datos Estructurales para laDefinición de Modelos Hidrogeológicos Conceptuales en Medios Fracturados.* Medellín: Universidad Nacional, Sede Medellín. Escuela de Geociencias y Medio Ambiente.

Gómez , E. (2019). Low Enthalpy Geothermal System at Dabeiba, Colombia; an Assessment Through the Hydrogeochemistry of Thermal Water. *Workshop on Geothermal Reservoir Engineerin. Stanford University.* , 2-6.

Gonzáles, H., & Londoño, A. C. (2003). *Geología de la Plancha 129 Cañasgordas - 145 - Urrao.* Medellín.: Memoria explicativa 119-Servicio geológico Colombiano.

Gorynski , K., Walker, D., Stockli , D., & Sabin, A. (2014). Apatite (U–Th)/He thermochronometry as an innovative geothermal exploration tool: A case study from the southern Wassuk Range, Nevada. *Journal of Volcanology and Geothermal Research 270*, 99-114.

Gorynski , K., Walker, J., Stockli, D., & Sabin, A. (2014). Apatite (U–Th)/He thermochronometry as an innovative geothermal exploration tool: A case study from the southern Wassuk Range, Nevada. *Journal of Volcanology and Geothermal Research 270* , 99–114.

Healy, R. W., & Cook, P. G. (2002). *Using groundwater levels to estimate recharge.* . Hydrogeology Journal. 10 (1), 91–109.

IGAC. (2007). *Cartografía de unidades de clasificación de suelo, Escala 1:100.000. 114 Dabeiba, Antioquia.* Medellín: Instituto geográfico Agustín Codazzi. SIG_Gobernación de Antioquia. .

Kenya, M., & Oham, N. (2009). *Application of geophysics to geothermal energy exploration and monitoring of its exploitation.* Lake Naivasha: KenGen P.O. Box 765.

Kresic, N., & Stevanovic, Z. (2010). *GROUNDWATER HYDROLOGY OF SPRINGS* . Burlington: Brithish Library-BH-USA.

Lerner, D. N., Issar, A. S., & Simmers, I. (1990). Groundwater recharge. A guide to understanding the natural recharge. *van Acken GmbH*, 245p.

Moeck, I. S. (2014). *Catalog of geothermal play types based on geologic controls.* Alberta: ELSEVIER- Renewable and Sustainable Energy Reviews 37 .

Nicholson , K. (1993). *Geothermal fluids: Chemistry and exploration techniques.* Berlin-Heidelberg: Springer 263.

(1993). *Nicholson K. Geothermal fluids: Chemistry and exploration techniques.* .

Powell , T., & Cumming, W. (2010). *Spreadsheets for Geothermal Water and Gas Geochemistry. Proceedings.* California: Thirty-Fifth Workshop on Geothermal Reservoir Engineering. Stanford University. PP 4-6.

Reed , M. J. (1982). *Assessment oflow-temperature geothermal resources of the United States.* Washington: USGS Circular 1983;892:73.

Rodríguez , G., & Arango , M. I. (2013). *Formación Barroso: Arco Volcánico Toleitico Y Diabasas De San José De Urama: Un Prisma Acrecionario T-Morb En El Segmento Norte De La Cordillera Occidental De Colombia.* Bogotá: Boletín Ciencias de La Tierra, 33, 17–38.

Rodríguez , G., & Zapata, G. (2012). *Características del plutonismo Mioceno superior en el segmento Norte de la Cordillera Occidental e implicaciones tectónicas en el modelo geológico del Noroccidente Colombiano.* Bogotá: Boletin de Ciencias de La Tierra, (31)- 5.22.

Rodriguez, G., Zapata, G., & Gomez , J. F. (2012). *Plancha Geológica 114, Dabeiba, Antioquia.* Medellín: Servicio geológico colombiano.

Roulleau , E., Bravo, F., Pinti, D., Barde-Cabusson , S., Pizarro, M., Tardani, D., . . . Morata, D. (2017). Structural controls on fluid circulation at the Caviahue-Copahue Volcanic Complex (CCVC) geothermal area (Chile-Argentina), revealed by soil

CO2 and temperature, self-potential, and helium isotopes. *Journal of Volcanology and Geothermal Research 341*, 104–118.

Schosinsky N, G. (2007). CÁLCULO DE LA RECARGA POTENCIAL DE ACUÍFEROS MEDIANTE UN BALANCE HÍDRICO DE SUELOS. *Revista Geológica de América Central, 34-35: 13-30, 2006 ISSN: 0256-7024*, 14-30.

Servicio Geológico Colombiano SGC. (2014). *Inventario nacional de fuentes termales-Reporte básico.* Medellín : Manantial Termal de Guineales (DABEIBA, ANTIOQUIA).

Servicio Geológico Colombiano SGC. (2014). *Inventario nacional de fuentes termales-Reporte básico.* Medellín: Manantial Termales de Chobar (DABEIBA, ANTIOQUIA).

Setyawan, A., Yudianto, H., Nishijama, J., & Hakim, S. (2015). *Horizontal Gradient Analysis for Gravity and Magnetic Data Beneath Gedongsongo Geothermal Manifestations Ungaran-Indonesia.* Melbourne: ELSEVIER.

Singhal, B., & Gupta, R. (2010). *Applied Hydrogeology of Fractured Rocks, Second Edition. .* Springer, 408 pp.

Sutter, F., Satori, M., Neuwerth, R., & Gorin, G. (2008). *Structural imprints at the front of the Chocó-Panamá indenter: Field data from the North Cauca Valley Basin, Colombia.* Tectonophysics, 460 (1–4).